Laia Mallol Bordas

Analysis of different Heuristic Methods for Cranial Point Localization: Assessing Accuracy Against the International 10/20 System

Final Degree Project

directed by Dr. Albert Fabregat Sanjuan

directed by Dr. Vicenç Pascual Rubio

Bachelor's Degree in Biomedical Engineering

UNIVERSITAT ROVIRA I VIRGILI

Tarragona
2024

Acknowledgements

I would like to begin by expressing my sincere gratitude to everyone who has supported me throughout this journey.

I am especially thankful to my supervisors, Dr. Albert Fabregat Sanjuan and Dr. Vicenç Pascual Rubio, as well as the members of the research group, Rosa Pàmies and Agnès Rigo, for their invaluable dedication, guidance, expertise, and constant support throughout this project.

Finally, I am deeply grateful to my family, my partner, friends, and university companions. Their unwavering support, patience, and encouragement helped me during this process, and I truly appreciate their belief in me.

Abstract

This study evaluates the accuracy of heuristic methods for cranial point localization compared to the International 10/20 System, with a focus on head morphology variations. A sample of 250 head models (125 female, 125 male) was obtained from the HumanShape website, featuring realistic measurements of Head Circumference (HC), Nasion-Inion (Ns-In), and Tragus-Tragus (LPA-RPA) distances. A Python script in FreeCAD was developed to automate cranial point localization. The heuristic methods studied include BeamF3, Adjusted BeamF3, the 5-7 cm method for locating CP3 and CP4, updated scalp heuristics for DLPFC localization, and methods for Kocher's point. The results indicate that while approximate methods provide a practical and quick alternative, significant discrepancies can occur depending on individual head measurements. The EPlacement device demonstrated consistent and reliable results across various head shapes, suggesting it could standardize and improve the accuracy of cranial point localization in clinical practice.

Keywords: cranial point localization, heuristic methods, International 10/20 System, head morphology, Head Circumference (HC), Nasion-Inion (Ns-In), Tragus-Tragus (LPA-RPA), FreeCAD, EPlacement.

Resum

Aquest estudi avalua l'exactitud dels mètodes heurístics per a la localització de punts cranials en comparació amb el Sistema Internacional 10/20, amb un enfocament en les variacions de la morfologia cranial. S'ha obtingut una mostra de 250 models de cap (125 femenins i 125 masculins) des del lloc web HumanShape, amb mesures realistes de perímetre cranial, distàncies Nasion-Inion (Ns-In) i Tragus-Tragus (LPA-RPA). S'ha desenvolupat un script amb el llenguatge Python a FreeCAD per automatitzar la localització de punts cranials. Els mètodes heurístics estudiats inclouen BeamF3, BeamF3 ajustat, el mètode de 5-7 cm per a localitzar CP3 i CP4, heurístiques actualitzades del cuir cabellut per a la localització del DLPFC i mètodes per localitzar el punt de Kocher. Els resultats indiquen que, encara que els mètodes aproximats proporcionen una alternativa pràctica i ràpida, poden ocórrer discrepàncies significatives segons les mesures individuals del cap. L'eina EPlacement ha demostrat resultats consistents i fiables a través de diverses formes de cap, suggerint que podria estandarditzar i millorar l'exactitud de la localització de punts cranials en la pràctica clínica.

Paraules clau: localització de punts cranials, mètodes heurístics, Sistema Internacional 10/20, morfologia del cap, perímetre cranial, Nasion-Inion (Ns-In), Tragus-Tragus (LPA-RPA), FreeCAD, EPlacement.

Index

Table of Figures

List of Tables

1 Introduction

The accurate positioning of electrodes on the scalp is crucial in various neurophysiological procedures, such as electroencephalography (EEG), repetitive transcranial magnetic stimulation (rTMS), evoked potentials (EPs), or even surgery. Individualized electrode placement is essential due to the anatomical variability of human heads, which can significantly impact the accuracy of neurophysiological measurements. The most widely used method for electrode placement in clinical practice is the International 10/20 System, which provides a standardized approach.

However, the 10/20 method has some disadvantages, particularly when performed manually. The process requires using a tape measure and calculating percentages, which can introduce inaccuracies and is time-consuming. Incorrect electrode placement can lead to erroneous patient results, adding further risk. On the other hand, while neuronavigation offers greater accuracy, it is a slow and expensive process, making it impractical for routine use in most medical settings due to its cost and complexity.

In clinical practice, approximate methods are often used to locate cranial points more quickly. This study will focus on evaluating several of these heuristic methods, including the BeamF3 method, updated scalp heuristics for localizing the dorsolateral prefrontal cortex (DLPFC), the 5-7 cm method for localizing CP3 and CP4, and the heuristic method for localizing Kocher's point.

This Final Degree Project aims to analyze the magnitude of positioning errors between the approximate methods and the 10/20 System based on cranial morphology, and it will propose alternatives to improve electrode placement and, consequently, enhance the accuracy of the technique using the EPlacement device, thereby facilitating the task of healthcare personnel.

To achieve the objectives of this study, the following steps were undertaken:

- **Obtaining head models**: A sample of 250 realistic head models was obtained from the HumanShape website. Parameters were varied to achieve realistic measurements of Head Circumference (HC), Nasion-Inion distance (Ns-In), and Left Preauricular – Right Preauricular distance (LPA-RPA) that represent the population.

- **Automating Cranial Point Localization based on the 10/20 International System**: Anatomical point detection and cranial points localization on each head model was automated by developing a Python script using a 3D design software Computer-Aided Design (CAD), specifically FreeCAD.

- **Analysis of different Heuristic Methods for Cranial Point Localization:** Comparison between different Heuristic methods and reference points from international 10/20 System was done for different positions (F3/F4, CP3/CP4, FFC3h/FFC4h).

- **Statistical analysis**: A statistical analysis was performed to quantify the positioning errors of the heuristic methods used in clinical practice.

1.1 The brain and neurons

The brain is the most complex organ in the human body, forms the central nervous system (CNS) with the spinal cord. It controls motor skills, thought, touch, memory, vision, emotion, breathing, hunger, temperature, and every process that regulates the body [1]. Neurons, the brain's fundamental units, are specialized, excitable cells that transmit information through electrical and chemical signals. Neurons communicate at synapses, where the axon terminal of one neuron connects with the dendrite of another. Neurotransmitters travel across the synaptic gap and attach to receptors on the receiving neuron.

Neurons communicate through electrical impulses known as action potentials [2]. When an action potential reaches the axon terminal, it triggers the release of neurotransmitters into the synaptic gap between neurons. These neurotransmitters bind to receptors on the postsynaptic neuron, allowing ions to flow across the membrane, which can either excite or inhibit the generation of a new action potential. The balance between excitatory and inhibitory inputs in a neuron determines whether a new action potential will be triggered. Action potentials are fundamental for neuron communication and occur when the sum of excitatory and inhibitory signals causes the membrane potential to reach a threshold, typically around -50 or -55 mV. These are the Action Potential Phases [3]:

1. Resting Potential (-70 mV): The membrane is at rest, dominated by K+ permeability, with K+ channels open and Na+ channels closed.
2. Threshold (-55 mV): A stimulus must reach this level for the neuron to trigger an action potential.
3. Depolarization (+30 mV): Rapid Na+ influx through open Na+ channels cause the membrane potential to become positive.
4. Repolarization: Na+ channels close, and K+ channels open, leading to K+ outflow and a return towards negative potential.
5. Ion Gradient Restoration: The Na+/K+ pump restores ion balance, moving 3 Na+ out and 2 K+ in.
6. Hyperpolarization (-80 to -90 mV): Continued K+ outflow makes the membrane potential temporarily more negative than the resting state.
7. Return to Resting Potential (-70 mV): The membrane returns to its resting state, ready for the next action potential.

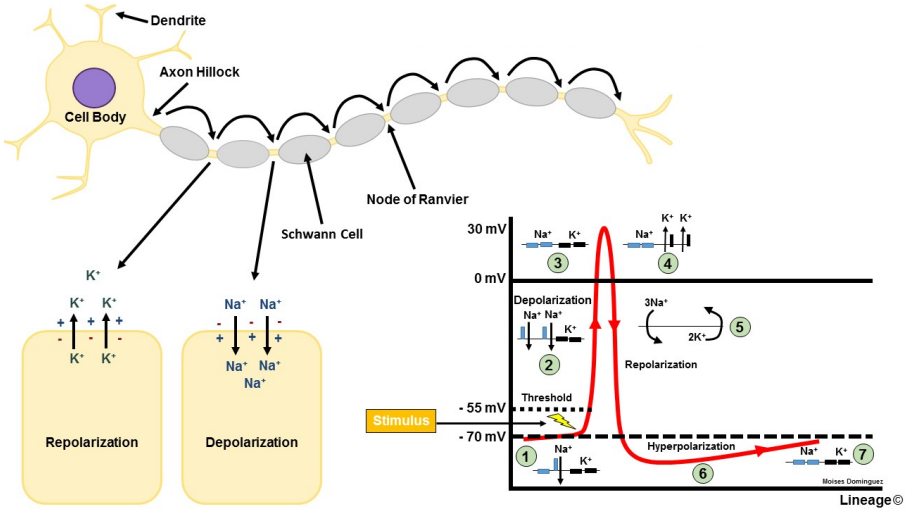

Figure 1 Neuronal Action Potential [Source: Action Potential Basics, 2022, https://step1.medbullets.com/neurology/113052/action-potential-basics]

1.1.1 Parts of the Brain and Their Functions

The brain can be divided into three main parts: the cerebrum, the cerebellum, and the brainstem. Each of these regions has distinct structures and functions [1], [4].

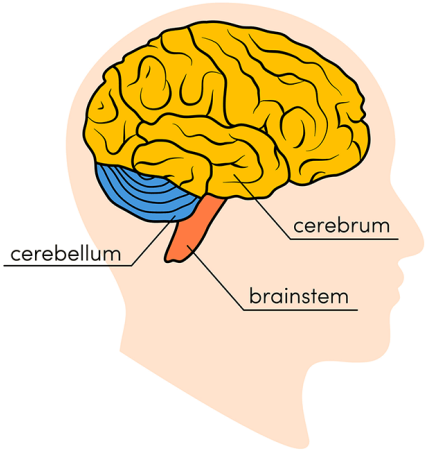

Figure 2 Parts of the Brain [Source: Anatomy of the Brain, 2024, https://www.hopkinsmedicine.org/health/conditions-and-diseases/anatomy-of-the-brain]

Cerebrum

Located at the front of the brain, is the largest part and consists of gray matter (the cerebral cortex) and white matter at its center. It is responsible for initiating and coordinating movement, regulating temperature, and processing sensory information related to vision, hearing, touch, and other senses. The cerebrum also plays a crucial role in higher cognitive functions such as speech, judgment, thinking, reasoning, problem-solving, emotions, and learning.

- Cerebral Cortex: The outer layer of the cerebrum, known as the cerebral cortex, has a large surface area due to its folds and accounts for about half of the brain's weight. It is divided into two hemispheres: the right hemisphere controls the left side of the body, and the left hemisphere controls the right side.
    - Sulci and gyri form the convolutions on the cerebral cortex [5]. These convolutions increase the brain's surface area, allowing for more neurons and complex functions. Gyri are the raised areas, while sulci are the grooves between them. This folding pattern helps fit the large cerebral cortex within the skull.

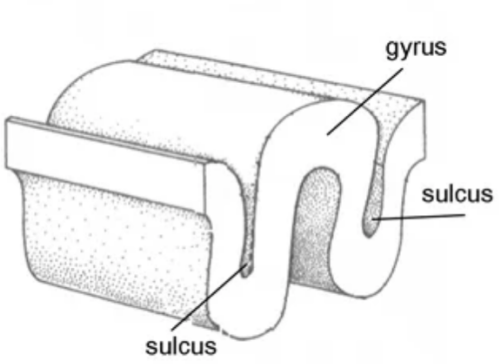

Figure 3 Sulcus and gyrus [Source: Gyri and Sulci of the Brain, 2023, https://www.simplypsychology.org/gyri-and-sulci-of-the-brain.html]

Cerebellum
Situated at the back of the head, beneath the temporal and occipital lobes and above the brainstem. It consists of two hemispheres and controls voluntary muscle actions, supports posture, and helps with balance and equilibrium. Neurons are found in the outer part, while the inner region connects with the cerebral cortex.

Brainstem
The brainstem serves as a connector linking the cerebrum and cerebellum to the spinal cord. It consists of the midbrain, pons, and medulla, where the spinal cord connects with the brain. It carries out numerous involuntary actions like breathing, heart rate, maintaining body temperature, sleeping, digestion, and reflexes such as sneezing, coughing, and swallowing.

1.1.2 Lobes of the Brain and What They Control

The cerebrum is divided into four lobes: frontal, parietal, temporal, and occipital [6]. Each lobe is responsible for different functions essential to human behavior, cognition, and sensory processing.

Frontal lobe
Located at the front of the brain, it is the largest lobe and is key for higher cognitive functions, motor control, and personality. It controls voluntary movements through the primary motor cortex and is involved in decision-making, planning, and smell recognition.

Parietal lobe
Situated behind the frontal lobe, it is essential for interpreting sensory information like touch and pain, understanding spatial relationships, and identifying objects. It also plays a crucial role in comprehending spoken language.

Occipital lobe
The occipital lobe is located at the back of the brain, in the posterior part of the cerebrum. It is dedicated primarily to visual processing. This lobe receives and interprets visual stimuli from the eyes, allowing individuals to perceive and understand visual inputs such as shapes, colors, and movements.

Temporal lobe
The temporal lobe is located on the sides of the brain. Is involved in short-term memory, speech, musical rhythm, and some degree of smell recognition.

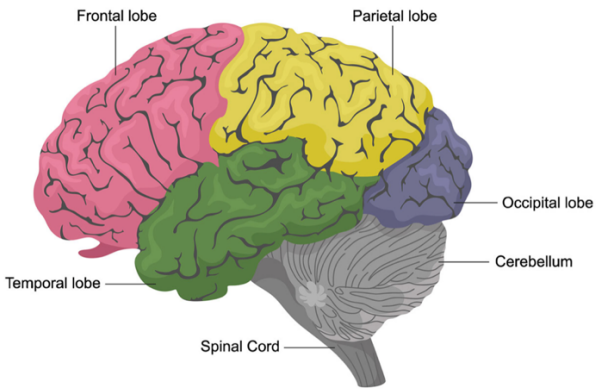

Figure 4 Lobes of the Brain [Source: Anatomy of the Brain, 2024, https://www.hopkinsmedicine.org/health/conditions-and-diseases/anatomy-of-the-brain]

1.2 Clinical Neurophysiology

Clinical Neurophysiology is a medical specialty focused on studying and diagnosing disorders of the central and peripheral nervous systems [7]. It utilizes techniques such as electroencephalography (EEG), polysomnography, evoked potentials (EPs), intraoperative neurophysiological monitoring (IONM), and repetitive Transcranial Magnetic Stimulation (rTMS), and even surgery, to record electrical or magnetic activity of the nervous system and to perform certain treatments. These techniques are essential for diagnosing, monitoring, and treating neurological diseases and are valuable across various medical fields, making Clinical Neurophysiology a central service in healthcare.

1.2.1 Clinical Neurophysiology Tests

Electroencephalography

Electroencephalography (EEG) is a medical test that measures brain's electrical activity in a non-invasive way. During an EEG, electrodes are placed on the scalp to detect electrical signals produced by neurons. These signals are then amplified and recorded as wavy lines on a computer screen or paper.

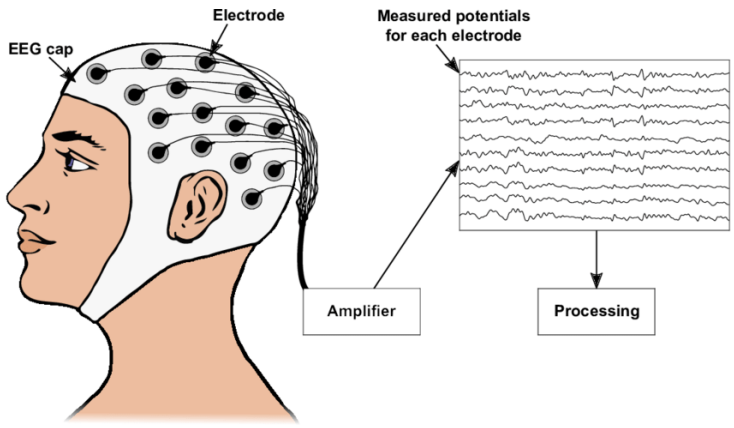

Figure 5 Sketch of how to record an EEG [Source: Towards a Home-Use BCI: Fast Asynchronous Control and Robust Non-Control State Detection, 2020, https://www.researchgate.net/publication/338423585_Towards_a_home-use_BCI_fast_asynchronous_control_and_robust_non-control_state_detection/figures]

Evoked potentials (EPs)

- Somatosensory EPs for upper and lower limbs: involve recording brain activity in the sensory cortex in response to electrical stimulation of the median or ulnar nerve (upper limbs) or the posterior tibial or femoral cutaneous nerve (lower limbs).

- Visual EPs: It involves recording the responses of the visual cortex to a visual stimulus.

- Auditory EPs: It involves recording auditory evoked responses to a "click" sound stimulus.

- Cognitive EPs: measures the brain's electrical responses to specific cognitive stimuli, such as auditory, visual, or sensory signals that require some level of cognitive processing [8].

Polysomnography:

Polysomnography, also known as a sleep study, is a test used to diagnose sleep disorders. It records brain waves, blood oxygen levels, heart rate, and respiratory rate during sleep. Additionally, it monitors eye and leg movements [9]. The test involves recording the brain's bioelectrical activity during wakefulness and light sleep using a custom-fitted cap with electrodes.

Intraoperative Neurophysiological Monitoring (IONM):

During surgery, Intraoperative neurophysiological monitoring (IONM) is used to evaluate the condition of neural structures and level of consciousness. It involves continuous monitoring of neural tissue and the localization of critical neural structures. The goal of IONM is to detect intraoperative neural damage early, allowing for timely intervention to prevent or minimize irreversible neurological damage and avoid postoperative deficits [10].

Repetitive Transcranial Magnetic Stimulation (rTMS):

Repetitive transcranial magnetic stimulation (rTMS) is a secure and non-intrusive treatment option for a range of psychiatric and neurological conditions. It works by applying high and low-intensity magnetic fields to stimulate specific deep brain regions, thereby modulating cortical excitability. This approach is reviewed for its efficacy in treating conditions such as treatment-resistant depression, PTSD, OCD, Tourette syndrome, and various movement disorders [11]. The optimal cortical target for the rTMS is the left prefrontal cortex [12], being the F3 location from the International 10/20 system the used by clinicians.

Surgery:

In brain surgery, a ventriculostomy is a common procedure to drain excess cerebrospinal fluid from the brain [13]. An intraventricular catheter is inserted to drain the fluid from the anterior horn of the lateral ventricle, with the entry point located on the frontal bone at a site known as Kocher's point [14].

1.2.2 Clinical Neurophysiology Tests and Electrode Locations Required

Each of these clinical tests requires the use of specific electrode placements. Below is a diagram illustrating the electrode locations according to the 10/10 and 10/20 International Systems used for each type of test.

This diagram is provided by the research group "*Grup NeuroÈpia*" of the "*Institut d'Investigació Sanitària Pere Virgili*".

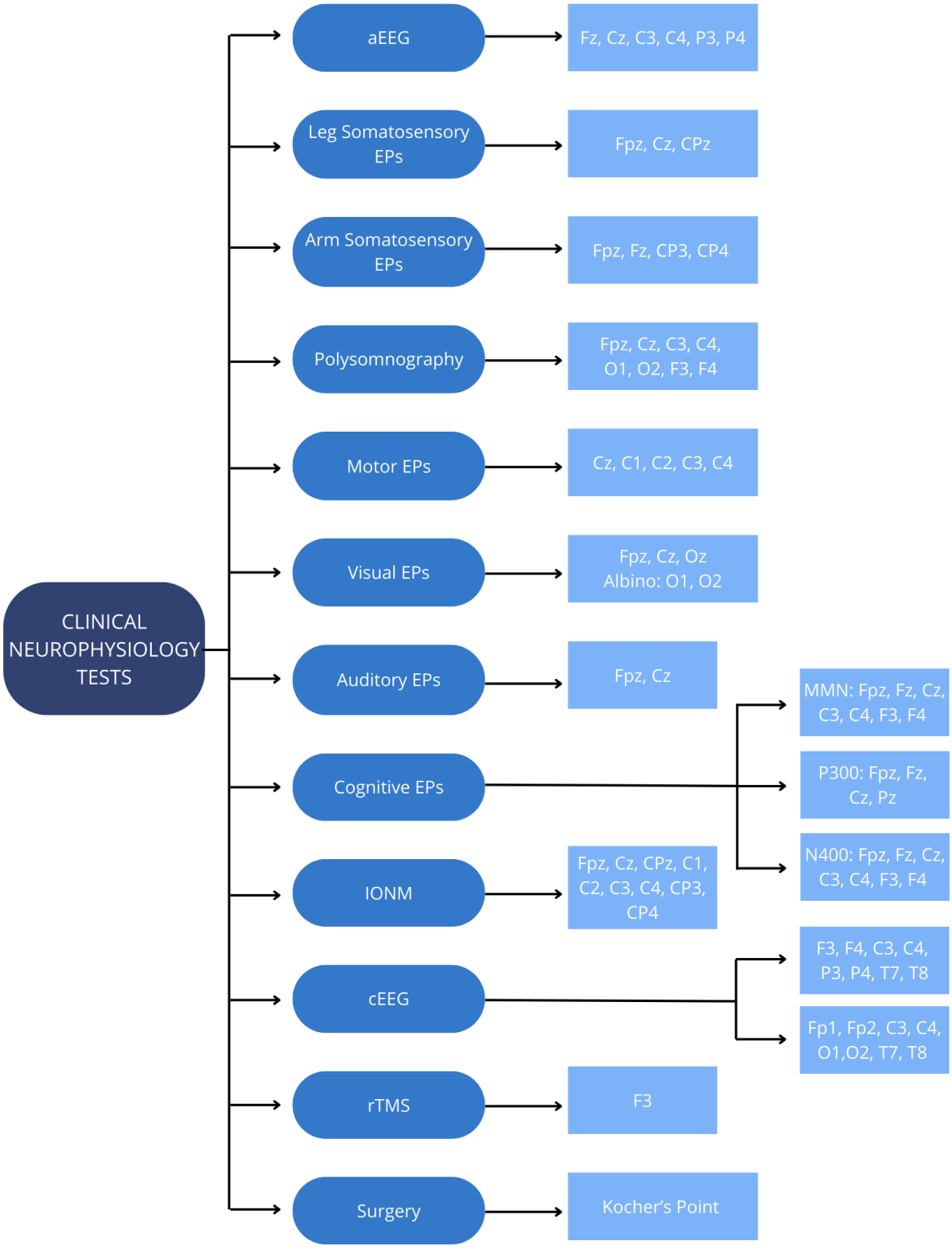

Figure 6 Diagram of Clinical Neurophysiology Tests and Electrode Locations Required [Source: Institut d'Investigació Sanitària Pere Virgili, 2024]

1.3 Heuristic Methods for Cranial Point Localization

1.3.1 International 10/20, 10/10 and 10/5 systems

The international 10/20 system has been the standard method for electrode placement in electroencephalography (EEG) for half a century. The primary purpose of the 10/20 system (Jasper, 1958) was to offer a consistent method for placing a relatively small number of EEG electrodes, typically 21, across different studies. However, the 10/20 system's primary use began to shift, starting to be used in direct positional guidance for newly developing techniques such as transcranial neuroimaging or transcranial magnetic stimulation [15].

This system identifies head surface locations by measuring the relative distances between cranial landmarks across the head's surface. The principles of this method specify that two adjacent electrodes are placed at distances of either 10% or 20% of the total distances between the Nasion-Inion, Tragus-Tragus or Head Circumference points on the skull [16] .

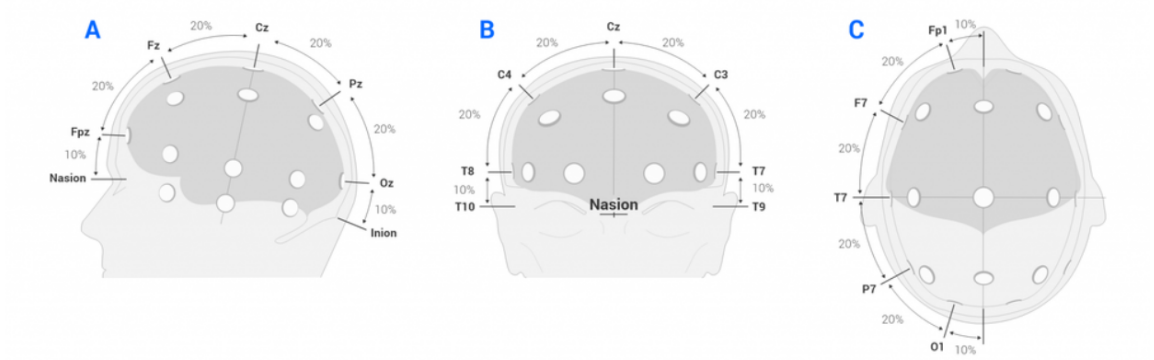

Figure 7 Placement of electrodes International 10/20 System [Source: La serie de electrodos estandarizados del EEG del IFCN. Neurofisiología clínica, 128(10), 2070-2077, 2017, https://www.bitbrain.com/es/blog/colocacion-electrodos-eeg]

The positioning of the electrodes is associated with the area of the cerebral cortex underlying it. The placements of the frontal, temporal, central, parietal, and occipital regions are denoted by the letters F, T, C, P, and O, respectively. The even numbers (2, 4, 6, 8) refer to electrode positions on the right hemisphere, the odd numbers (1, 3, 5, 7) on the left hemisphere and the 'z' refers to electrode placement in the sagittal plane [17].

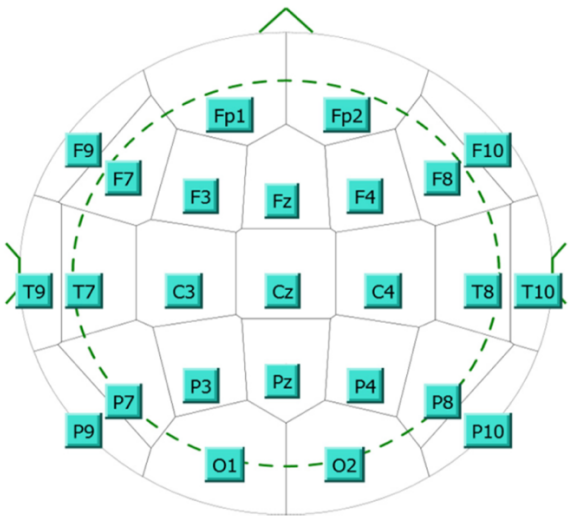

Figure 8 The International 10/20 System [Source: The standardized EEG electrode array of the IFCN, 2017, http://medi-guide.meditool.cn/ymtpdf/5CCE28C2-AC7E-123E-084D-A277020B6472.pdf]

With the emergence of multi-channel EEG hardware systems and simultaneous advancements in topographic and tomographic signal source localization methods, there was an increased need to expand the 10/20 system to higher density electrode settings. As a result, the **10/10 system** was introduced as an extension of the original 10/20 system, featuring a higher channel density of 81 electrodes (Chatrian et al., 1985) [15]. This system is obtained by dividing each of the 20% percentages to a 10%.

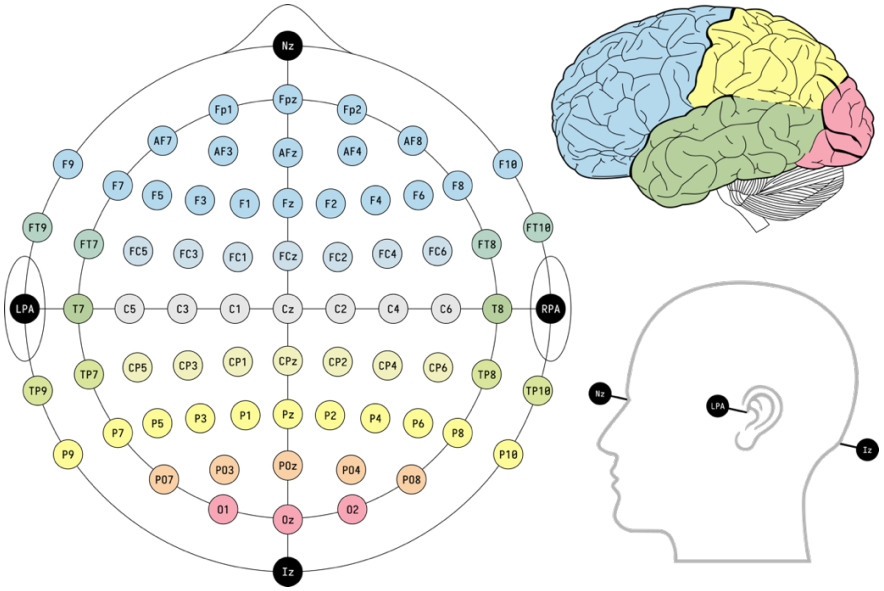

Figure 9 International 10/10 System [Source: EEG 10-10 system with additional information, 2023, https://commons.wikimedia.org/wiki/File:EEG_10-10_system_with_additional_information.svg]

However, even higher density electrode settings were desired. Consequently, the 10/10 system was extended to the **10/5 system** (Oostenveld and Praamstra, 2001) [15]. By dividing the percentages to a 5%, the use of more than 300 electrodes was enabled.

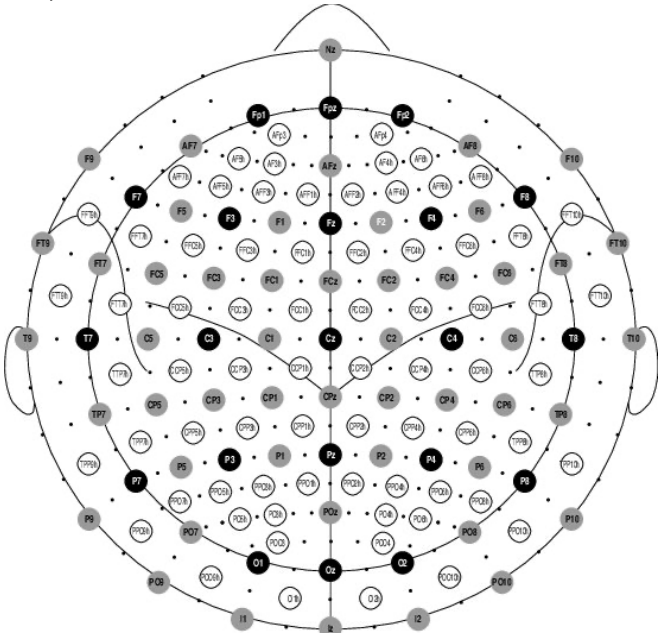

Figure 10 International 10/5 System [Source: Improving EEG source analysis using prior knowledge, 2003, https://www.researchgate.net/publication/254876989_Improving_EEG_source_analysis_using_prior_knowledge]

1.3.2 BeamF3 method

The Beam F3 System is a simplified method designed to locate the F3 position on the scalp. It is important to note that the Beam F3 method imposes two assumptions: (i) the location of F3 is at the intersection between the Fz-F7 and C3-Fp1 lines, and (ii) the angle of the polar coordinates of Fz, F7, C3, and Fp1 is fixed, meaning it does not change with head shape [18]. Unlike the traditional International 10–20 system, which involves numerous measurements and calculations, the Beam F3 System streamlines the process using only three skull measurements and a computer program [19]. This innovation makes the procedure faster and reduces the potential for human error [20].

Figure 11 Beam F3 Location system in practice [Source: An efficient and accurate new method for locating the F3 position for prefrontal TMS applications, 2009, https://pubmed.ncbi.nlm.nih.gov/20539835/]

The three required measurements are: the distance from the nasion to the inion, the distance between the left and right preauricular points, and the head circumference. These measurements are used to identify the vertex on the scalp, where the halfway points of the nasion-inion and preauricular distances intersect. Once these values are obtained, they are entered into a computer program, which then calculates the precise location of F3 by providing two output values (X and Y) that specify the distance from the vertex.

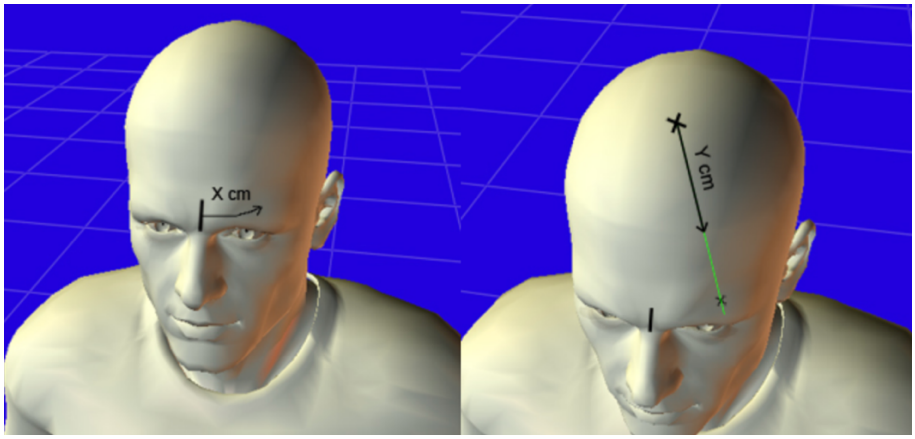

Figure 12 BeamF3 software used to facilitate calculations [Source: Will Beam & Jeff Borckardt Web Interface, Developed 6/7/2010, https://clinicalresearcher.org/F3/calculate.php]

To locate the F3 position, a point along the head's circumference is marked X cm from the midline. This point serves as a reference for the next step. Then, F3 is identified as a point along a line running from the vertex (the top "x" on the head) through the previously marked point, Y cm from the vertex.

Adjusted Beam F3

Mir-Moghtadaei et al. (2015) [21], did a study to compare the BeamF3 heuristic, with MRI-guided neuronavigation, which targets a specific DLPFC coordinate. Using 100 pre-treatment MRIs, researchers found that the discrepancies between BeamF3 and MRI-guided sites were less than 0.65 cm in 50% of subjects, less than 0.99 cm in 75%, and less than 1.36 cm in 95%. While the angle from the midline did not significantly differ between methods, the radial arc length was slightly longer (0.35 cm) with MRI-guidance. These findings suggest that the BeamF3 heuristic approximates MRI-guided neuronavigation for the left DLPFC in most subjects and adjusting the distance from the vertex adding 0.35 cm to the result could further enhance its accuracy.

1.3.3 Updated Scalp Heuristics for localizing the DLPFC

With the objective of creating an updated scalp heuristic for localizing the DLPFC, Siddiqui et al. (2021) [22] developed a brain map through independent, yet convergent analyses of the functional networks associated with response and non-response to procedures applied to the dorsolateral prefrontal cortex (DLPFC). New stimulation sites in the DLPFC are identified through a merging multimodal analysis involving brain stimulation (rTMS and DBS) and brain lesion mapping to determine brain circuits containing nodes that could help in the treatment of depression. The resulting map identified two foci of interest in each hemisphere, proximal to F3 and F4. Building on this finding, Mir-Moghtadaei et al. (2022) modified the BeamF3 heuristic using the MNI ICBM152 anatomical template to better estimate the DLPFC target site for stimulation, resulting in an updated set of scalp-based heuristics that localize the sites closest to the four foci of interest identified by Siddiqui et al. (2021).

From the measurements Nasion – Inion (NI), Tragus – Tragus (TrTr) and Head Circumference, they derived equations to calculate the arc length for four key DLPFC targets: left and right anterior (LA and RA) DLPFC, and left and right posterior (LP and RP) DLPFC. The equations are as follows:

- LA DLPFC:
  - $Y = ((NI + TrTr) / 2) * 0.3167$ (Eq. 1)
  - $X = HC * 0.1359$ (Eq. 2)
- RA DLPFC:
  - $Y = ((NI + TrTr) / 2) * 0.2884$ (Eq. 3)
  - $X = HC * 0.1352$ (Eq. 4)
- LP DLPFC:
  - $Y = ((NI + TrTr) / 2) * 0.2480$ (Eq. 5)
  - $X = HC * 0.1847$ (Eq. 6)
- RP DLPFC:
  - $Y = ((NI + TrTr) / 2) * 0.2316$ (Eq. 7)
  - $X = HC * 0.1968$ (Eq. 8)

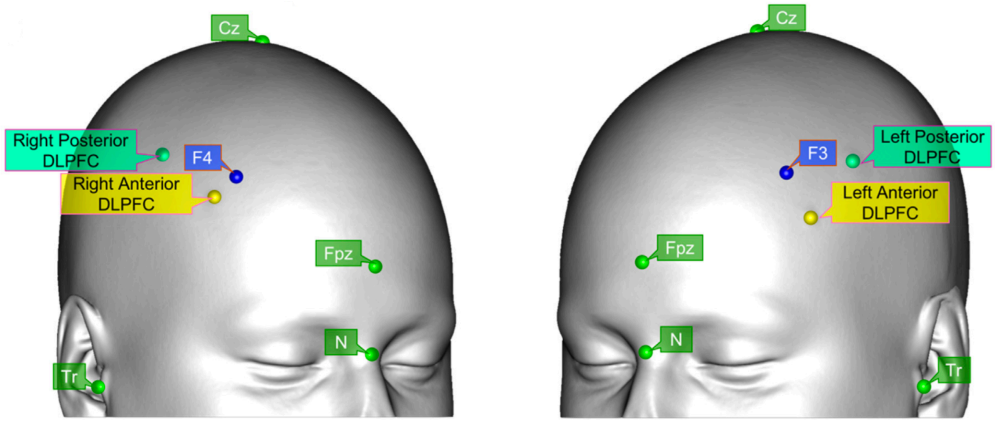

Figure 13 Updated Scalp Heuristics for localizing DLPFC [Source: Updated scalp heuristics for localizing the dorsolateral prefrontal cortex based on convergent evidence of lesion and brain stimulation studies in depression. Brain Stimulation, 15(2), 291–295, 2022, https://doi.org/10.1016/j.brs.2022.01.013]

Among these newer sites, the LA-DLPFC was 21.5 ± 1.4 mm more inferior-posterior to F3 (geodesic distance along scalp surface), while the LP-DLPFC is 37.0 ± 0.6 mm more posterior. Similarly, the RA-DLPFC is 12.3 ± 0.9 mm more inferior-posterior to F4 while the RP-DLPFC is 44.1 ± 0.9 mm posterior.

1.3.4 Method 5 – 7 cm for localizing CP3 and CP4

This is a heuristic method used by clinical neurophysiologist in their usual practice, to locate the CP3 and CP4 points from the international 10/10 system. The method involves measuring 5 cm posterior to the Cz point and then moving 7 cm laterally towards the tragus. This technique provides a practical way to locate the CP3 and CP4 points, used in Somatosensory Evoked Potentials.

1.3.5 Kocher Point

Kocher's point serves as a frequent site of entry for an intraventricular catheter through the frontal bone. This point is located approximately 11 cm posterior to the nasion, and 3 centimeters lateral to the midline, at approximately the mid-pupillary line [23].

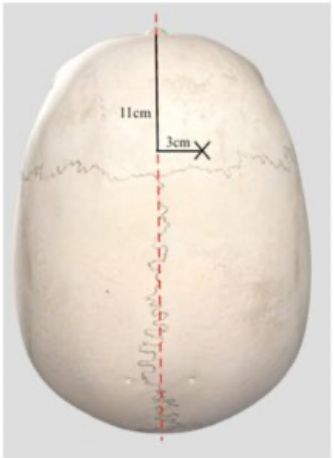

Figure 14 Kocher's Point Localization [Source: The Evolution of the Role of External Ventricular Drainage in Traumatic Brain Injury, 2019, https://www.mdpi.com/2077-0383/8/9/1422]

This point is also located 2 cm anterior to the coronal suture along the mid-pupillary line [24], as used by neurosurgeons to drain the cerebral ventricles in situations of severe intracranial hypertension.

1.4 EPlacement

In clinical practice, cranial points are located by performing percentage calculations based on numerical values obtained using a tape measure. With the aim of creating a device that avoids the inaccuracy and inconvenience of working with a tape measure, the EPlacement device was developed to offer a fast, simple, and accurate method for determining the location of cranial points during neurophysiological studies [25]. The EPlacement device was developed by the research group "*NeuroÈpia*" by the Dr. Albert Fabregat and Dr. Vicenç Pascual and is intellectually protected by an international patent [26]. The device substitutes the conventional Tape measure (TM) marking procedure or advanced systems such as neuronavigation or 3D scanners. More information about EPlacement can be found in the final degree project from Agnès Rigo [26] and the paper in which the accuracy and comparison with tape measurements are done [27] .

The device consists of several key components: an electronic unit that includes a display, a microcontroller, and a battery; a pressure sensor; and an illumination system with a high density of LEDs. The electronic unit is particularly user-friendly, featuring a navigation menu that allows clinicians to easily select the appropriate test for the procedure being performed. Two different versions of the EPlacement device were designed. The first version consists of a single strip (1S-EP) and the second one comprises two strips (2S-EP) that allow movement between them.

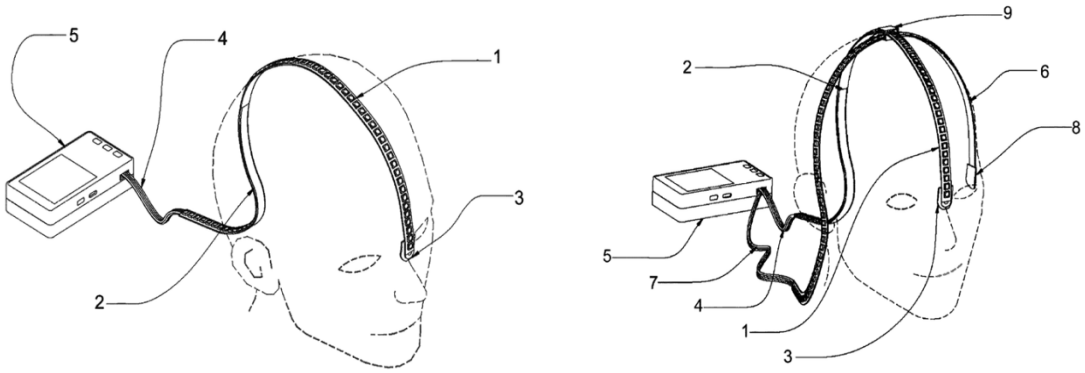

Figure 15 EPlacement device 1S-EP (left) and 2S-EP (right) [Source: [26]]

The marking process begins by obtaining the LPA – RPA distance and the Nasion – Inion (Ns-In) distance, by marking them with a touch sensor and confirmed with LED lighting. In the case of 2S-EP one strip is located at the tragus reference points and the second strip at the nasion and inion points. Then, the microprocessor calculates the distances and illuminates the point Cz where the strips have to intersect. Once the Ns-In and the LPA-RPA lines are marked, if more points are needed, the Ns-In trip can be rotated, and more points illuminated. Finally, the results can be exported.

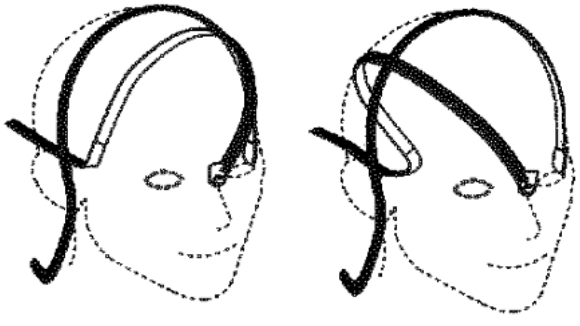

Figure 16 Nasion-Inion EP strip rotated [Source: [26]]

2 Methods and materials

2.1 Human Shape

To acquire a sample of realistic human heads, the Head Shape Model from the realistic human body shape modeler *Human Shape* [28] was used. This modeler was developed by the University of Michigan Transportation Research Institute. The models are based on statistical analyses of high-resolution laser scans and anthropometric measurement data of men, women, and children with a wide range of age, stature, and body weight. This body shape generator not only offers male and female head shapes, but also shapes for seated or standing children, toddlers, and adults.

This web presents a parametric head shape model derived from a statistical analysis of a large sample of adult head scans, free from hair artifacts. These high-resolution scans of 180 adults, both female and male, were standardized using a template-based fitting method. Principal Component Analysis (PCA) and multivariate regression analysis were performed on the head geometry, incorporating 58 anatomical landmarks, 12 anthropometric dimensions, and demographic data of the subjects [29].

These 58 landmarks are crucial for aligning the scans to a uniform coordinate system and standardizing the mesh structure to ensure anatomical consistency across the scan data, which is essential for statistical analysis. The coordinate system was defined at the Frankfurt plane, which is a horizontal plane passing through left and right tragion and right infraorbital landmarks, given by:

- Origin: Mid-tragion (Mid-point between right and left tragions).
- Y(Medial-Lateral): Right tragion to left tragion.
- Z(Caudal-cephalad): Vertical; obtained as the cross product of the Y axis and the horizontal Frankfurt plane (passing through tragions and infraorbital).
- X(Anterior-Posterior): cross product of the Y and Z axes.

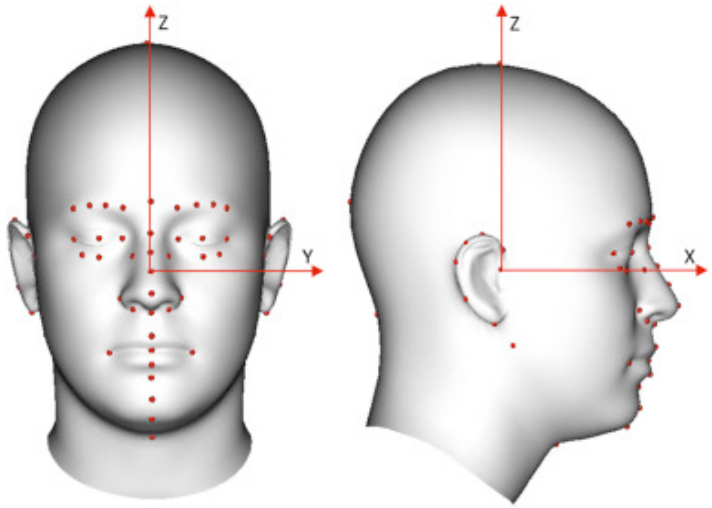

Figure 17 Coordinate System of HumanShape head models [Source: [28]]

The data source consisted of 180 adult 3D head scans, 100 female and 80 male, with ethnic diversity and a range of age from 18 to 59. The following tables show the ethnicity of the subjects and the head anthropometry descriptive statistics.

		MEAN	SD	MIN	MAX	5TH	95TH
MALE	Head Breadth (mm)	155.1	5.4	143.0	175.0	145.5	165.0
	Head Circ. (mm)	575.0	15.2	545.0	615.0	553.0	604.5
	Head Length (mm)	200.5	6.6	187.0	224.0	190.5	212.5
	Breadth-to-Length	0.77	0.03	0.71	0.84	0.72	0.84
	Age (YO)	35.6	9.3	19.0	56.0	22.0	52.5
FEMALE	Head Breadth (mm)	146.6	5.8	134.0	165.0	137.0	156.8
	Head Circ. (mm)	556.8	19.3	509.0	610.0	522.6	590.0
	Head Length (mm)	186.5	8.8	152.0	202.0	172.0	200.0
	Breadth-to-Length	0.79	0.04	0.70	0.96	0.72	0.86
	Age (YO)	27.7	10.2	18.0	59.0	19.0	50.8

Table 1 HumanShape Head anthropometry descriptive statistics (n=180)

Ethnicity/Race	Male	Female	Total
Asian/Pacific islander	2	14	16 (8.9%)
Black/African American	32	13	45 (25%)
White/Caucasian	33	65	98 (54.4%)
Hispanic	3	4	7 (3.9%)
Others	10	4	14 (7.8%)

Table 2 HumanShape: Ethnicity/race of the subjects

As mentioned previously, 12 head anthropometric dimensions were measured in each subject to supplement the information obtained from the head scans. Five of these dimensions were manually obtained, including Head Length, Breadth, Circumference, and Tragion to top of head, also the Length-Breadth Ratio. An additional seven dimensions were computed from the scans using an automatic dimension computation algorithm based on landmark locations. Table 3 lists the manually measured and digital head dimensions.

Standard manual head anthropometry	Head anthropometry estimated from 3D scans
Head Length	Bitragion Chin Arc
Head Breadth	Bitragion Submandibular Arc
Head Circumference	Bitragion Width
Length-Breadth Ratio	Head Arc Length
Tragion To Top-Of-Head	Face Width
	Ear Height
	Arc Width

Table 3 HumanShape: manually measured head anthropometry, and digital head dimensions estimated from 3D scans

The *Human Shape* web enables the generation of 3D head models by adjusting four parameters: Head Circumference (mm), Breadth to length Ratio, Bitragion Chin Arc (mm), and Tragion to Top (mm). Additionally, users can choose between male and female models.

2.1.1 Head Shape Parameters

- **Head circumference** (mm): the length of the intersection of the head surface and the plane perpendicular to the midsagittal plane, passing through the glabella and ophistokranion. The glabella is the point located at the middle of the eyebrows, and the ophistokranion is most posterior point of the occipital bone in the mid-sagittal plane. The range on the adjustable parametric bar is 500 – 650 mm.

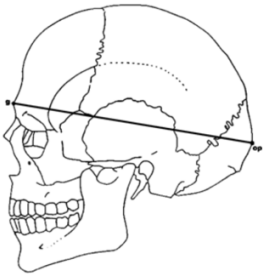

Figure 18 Head Circumference Plane [Source: Facial patterns and primary nocturnal enuresis in children, 2010, https://doi.org/10.1007/s11325-010-0388-6]

- **Breadth To Length Ratio** (BLR): also known as the cephalic index, it is calculated by multiplying the head breadth (HB) by 100 and dividing by the head length (HL). The HB is the greatest transverse diameter of the head, measured from euryon to euryon (bilaterally paired points that forms the terminus of the line of greatest breadth of the skull, not fixed points). The HL is the distance between the glabella and the opisthokranion [30]. The range on the adjustable parametric bar is 0.6 – 1.

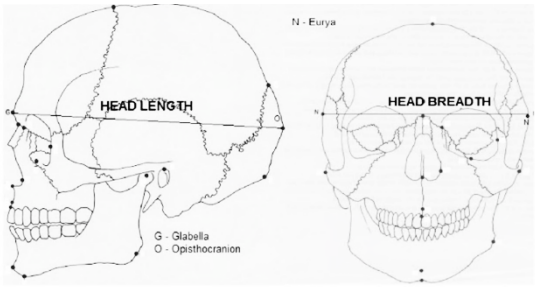

$$BLR = \frac{HB}{HL} \times 100 \qquad \text{(Eq. 9)}$$

Figure 19 Representation of Head Breadth and Head Length [Source:https://www.sciencedirect.com/science/article/pii/S2090536X16300752]

- **Bitragion Chin Arc** (mm): is the surface distance between the left and right tragion across the anterior point of the chin. The range on the adjustable parametric bar is 265 – 380 mm.

Figure 20 Representation of Bitragion Chin Arc [Source: https://humanshape.org/Updates.html]

- **Tragion to Top of the Head** (mm): is the vertical distance between the right tragion landmark and the horizontal plane tangent to the top of the head. The range on the adjustable parametric bar is 110 – 145 mm.

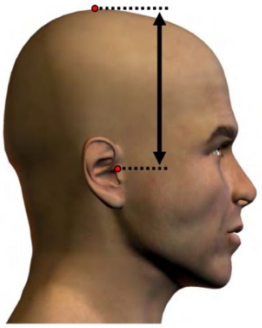

Figure 21Representation of Tragion to Top [Source: https://humanshape.org/Updates.html]

2.1.2 Landmarks used as anatomical points

When the Head model is downloaded from *HumanShape* a CSV file with the 58 landmarks and their coordinates can be obtained. This is very useful because later in the 3D analysis, some of them are used as anatomical points. Here is a list of which ones have been used along with their respective anatomical points:

- *Nose Sellion Center* defined by Human Shape as the deepest depression of the nasal bones at the top of the nose: **Nasion**.

- *Ear Tragion Right and Left* defined as the point located at the upper margin of each tragus: **Tragus** (LPA and RPA).

Since there wasn't any landmark that could be used for the Inion point, we reached out to *HumanShape* researchers, wondering if they could assist in our inquiries. They sent us a document containing the indices of the central vertices of the heads. We plotted these vertices and selected the one that would anatomically correspond to the inion. Thus, we identified vertex index 4697. Noting that these central vertices did not symmetrically divide the head, we are primarily interested in the Z coordinate of this vertex.

- Vertex 4697: the Z coordinate of this ID in each head, has been used as the Z coordinate of the **Inion** point.

To obtain the coordinate of the vertex 4697 in each head, a MATLAB code using the function readObj() was executed. This code added a line to the Landmarks CSV with the coordinates of the vertex 4697.

2.2 Sample of Human Head Models

The initial idea was to create a realistic sample of head shapes using a Design of Experiments (DOE) approach with a 5x5x5 matrix, based on HC, Ns-In and LPA-RPA, varying these parameters by ±sigma, ±2 sigma, and sigma. The problem is that HumanShape web does not work with these parameters, and the only matching parameter is HC, but the values entered in HumanShape did not match the measured HC. To address this, an attempt was made to develop equations that could correlate the parameters used by HumanShape with HC, Ns-In, and Tr-Tr. Unfortunately, the results were not as expected, with discrepancies of up to 3 cm between the predicted and actual measurements. As a result of these inconsistencies, it was decided to proceed using the parameters provided by HumanShape for the study.

The current study has a sample of n = 250 models of realistic human heads, 125 male and 125 female. These models were picked using a 5x5x5 DOE setup, focusing on head shape parameters in *HumanShape*. The features used are Head Circumference (HC), Breadth to Length Ratio (BLR) and Tragion to Top (TtTop). The fourth parameter Bitragion Chin Arc has been set to the medium (320 mm), because has no effect on the cranial morphology since it is the distance between the left and right tragion across the anterior point of the chin.

Percentile	HC	BLR	TtTop
5%	508	0.62	112
25%	539	0.70	119
50%	575	0.80	128
75%	614	0.90	136
95%	643	0.98	143

Table 4 HumanShape parameters used in the 5x5x5 DOE for the Human Head Models sample

The idea is to vary the parameters of *HumanShape* to obtain a realistic variability of head models. Specifically, to achieve the corresponding values of the three key parameters HC, Ns-In and LPA-RPA:

- **Head Circumference**: The values range from 526.2 to 624.4 mm.
- **Ns-In**: The values range from 324.8 to 414.9 mm.
- **LPA-RPA**: The values range from 333.1 to 405.2 mm.

Adjusting these parameters generates a diverse and representative set of head shapes that reflect the natural variability found in the human population. This approach ensures that the sample of 250 head models captures a broad spectrum of cranial morphologies. The ranges for these values are derived from the scalp-based measurements obtained by Mir-Moghtadaei et al. (2015) [31], from a sample of 100 subjects.

	Mean	SD	Minimum	Maximum
HC (mm)	573.1	23.4	526.2	624.4
Ns-In (mm)	363.2	17.4	324.8	414.9
LPA-RPA (mm)	365.1	15.3	333.1	405.2

Table 5 Representation of realistic variability of HC, Ns-In and LPA-RPA distances

2.3 FreeCAD

To work with the head models, a 3D design tool was necessary. FreeCAD is a 3D parametric modeling application, primarily made for mechanical design, but also serves other purposes where precision and controlled modeling are required. FreeCAD was chosen for this project because it supports the use of macros and scripts programmed in Python, allowing for greater flexibility and automation in the modeling process [32].

FreeCAD's scripting environment is a powerful feature that enhances its capabilities significantly. It includes an integrated Python console and supports the use of macros programmed in Python. A macro is a convenient way to reproduce complex actions in FreeCAD, and they are, in fact, a list of Python commands. You can do an action manually and by recording or using the Python console, you can obtain the line of code to replay this action whenever is needed [33].

The basic idea of the FreeCAD interface is that it is divided into workbenches. A workbench consists of tools designed for a particular purpose, such as working with meshes, drawing 2D objects, or creating constrained sketches. It is possible to change the current workbench using the workbench selector. Also, personalizing the tools found in every workbench by adding tools from different workbenches or developing custom tools known as macros. In this project, the workbenches used were Mesh, Draft, Part Design, Part, and Sketcher.

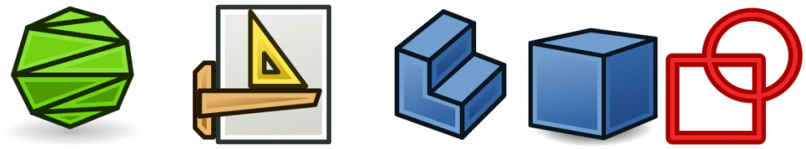

Figure 22 Icons of FreeCAD workbenches [Source: [32]]

- **Mesh**: the mesh workbench offers commands to directly manipulate meshes, for example: Import mesh or Create section from mesh and plane (the ones used in this project). The head shapes were imported to FreeCAD as a mesh object. A mesh is a type of object that defines 3D data, containing only vertices (points), edges and triangular faces [34]. Head objects downloaded from *Human Shape* have 5487 vertices.

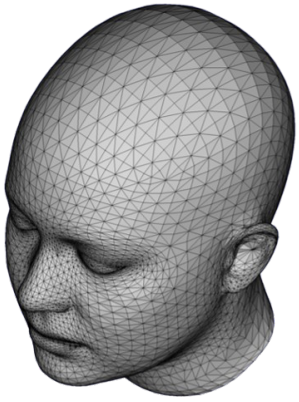

Figure 23 Head Mesh Object

- **Draft**: is focused on the creation and modification of 2D objects [35]. Some of the modification tools were the most used in this work:
    - Path Array: creates an array from a selected object by placing copies along the path. It was used to create an array with separated points from a B-spline and a point, such as the Nasion-Inion line with 11 points.
    - Draft to Sketch: it converts Draft objects to Sketches and vice versa. The main use was to convert sections (created by a plane and the mesh) to sketches, so they could be cut it. Also, this command converted Sketches to Wires.
    - Wire to B-spline: it converts Draft Wires to Draft B-Splines and vice versa. The B-splines created were used to make Path Arrays.

- **Part Design**: in this workbench the helper tools were used [36]:
    - Create a body: to create other datum, a Body object in the active document was required.
    - Create datum:
        - Create a datum plane: planes from 3 points.
        - Create a datum line: for example, from two points.
        - Create a datum point: from a draft point or the proximity point from two selected objects.

- **Part**: the planes created with the Part Design could not be used in the Mesh workbench, so the use of the Part workbench was required. The principal use was to Create primitive Planes placed and attached to the planes created in the Part Design.

- **Sketcher**: the Sketch edit mode was used to modify and cut the Sketches created in the Draft workbench.

2.3.1 Previous work to obtain the Final Python Macro in FreeCAD

Given the complexity of the procedure to manually obtain all the points and measurements explained in Annex 1, a Python macro to reproduce all the steps automatically on other heads is developed. Part of the script was designed by the "*Grup NeuroÈpia*" of the "*Institut d'Investigació Sanitària Pere Virgili*". I then worked on the code, adding new functionalities to cover all the necessary methods for the study.

The first structure of the procedure was:

- **Script Part 1**: it covers everything from the import of the mesh to the creation of the head circumference line.
- **Manual Step**: it involves the step of opening the sketch by a few μm or less to achieve a symmetrical Oz, and therefore symmetrical hemispheres.
- **Script Part 2**: it handles the rest of the steps, starting from the opened sketch to finding all the measurements and creating a Spreadsheet with all the important measures, which is downloaded as a CSV file.

Initially, the code used the "Head Top Center" landmark to create the plane that separates the two hemispheres. However, it was observed that the hemispheres were not symmetrical. The solution was to manually open the sketch of the head circumference and use this wire to create a path array of three points. This approach helped to achieve a symmetrical Oz and, consequently, symmetrical hemispheres.

Later, I noticed that while this method did produce totally symmetrical hemispheres, the lines between the points on the Nasion-Inion line and the points on the head circumference line were not symmetrical. In the following table, there is an example of a case where there was almost a 10 mm difference between the right and left sides of the head. To address this issue, I found a more symmetrical Top point.

In HumanShape, the origin is located between the two tragus points. Therefore, I created a path array of three points between the tragus points, with the middle point being considered the symmetrical top. Although this adjustment may result in a 1 mm difference between the hemispheres, it significantly improves the symmetry of the lateral lines. Additionally, by achieving symmetry through this symmetrical top point, the manual step in the script can be eliminated, ensuring that human factors do not impact the execution of the program.

TOP Landmark	Right (mm)	Left (mm)	Diff. (mm)
Hemispheres	293,93	293,93	0
AFz line	65,963	68,92	2,957
Fz line	97,77	103,2	5,43
FCz line	120,63	127,61	6,98
Cz line	132,13	140,69	8,56
CPz line	127,08	136,49	9,41
Pz line	103	112,37	9,37
POz line	66,08	71,38	5,3

TOP Tragus	Right (mm)	Left (mm)	Diff. (mm)
Hemispheres	293,335	294,504	1,169
AFz line	67,41	67,17	0,24
Fz line	100,99	100,05	0,94
FCz line	124,81	123,48	1,33
Cz line	136,74	136,1	0,64
CPz line	131,39	132,14	0,75
Pz line	106,34	108,96	2,62
POz line	67,9	69,35	1,45

Table 6 Left and Right hemisphere measurements using the Head Top Center Landmark and the symmetric top in the middle of the Tragus line

In addition to using the symmetrical top point and eliminating the manual step, my contributions to the code include adding the following:

- The implementation of the "Method 5-7 cm" for locating the CP3 and CP4 points.
- The identification and placement of the 5 Kocher points in each hemisphere (10 points in total).
- The EPlacement percentages for the points: CP3, CP4, CP3 5-7, CP4 5-7, P3, P4, FP1, FP2, O1, O2, K1 (L/R), K2 (L/R), K3 (L/R), K4 (L/R) and K5 (L/R).

Given that the Nasion-Inion plane is rotated relative to the XZ plane of the mesh, the transformation of the coordinates for all points is implemented by calculating the rotation angle and translation vector and applying them to the original coordinates.

All these additions have also been incorporated into the CSV file.

2.3.3 Python Macro to obtain the Cranial Points in FreeCAD automatically

In the following section you will find a step-by-step explanation of what the code does.

Import of the head mesh and creation of the landmark points

The head mesh document and the landmarks csv files path are introduced to the code. A new document is created, and the head mesh is imported. All the points from de csv file provided by HumanShape and the Inion ID coordinates, are created in the 3D file.

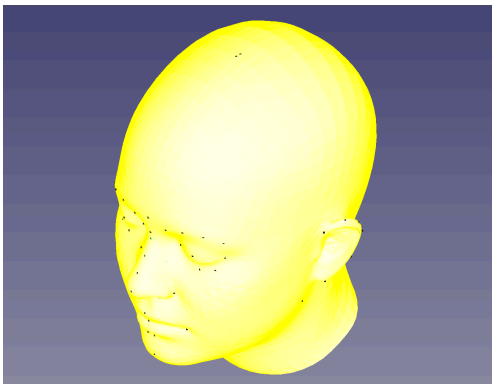

Figure 24 Steps Macro FreeCAD: Head Shape Model imported in FreeCAD

Identification of 3 anatomical points: Nasion, Inion and Tragus

The Nose Sellion Center landmark is used as Nasion and the Ear Tragion Left and Right as Tragus. To locate the Inion the first step is to create a plane parallel to the XY plane at the height of Z coordinate of the Inion of the ID. This plane is used to split the mesh and retain the upper part, by choosing the option "Above" in the dialog box displayed.

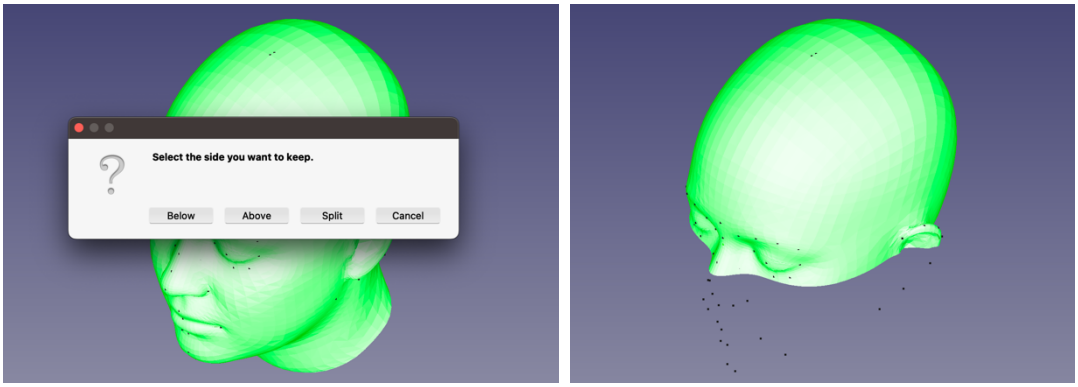

Figure 25 Steps Macro FreeCAD: First dialog box displayed and the mesh split

As explained before, a symmetrical top point is identified as the midpoint between the two Tragus. Vectors are then created from the origin to the Nasion and from the origin to this Top point. The cross product of these vectors is computed to obtain an orthogonal vector V. Using a vertex of the Nasion-Origin line and the orthogonal vector V, a plane is created to divide the right and left hemispheres of the head. This plane intersected with the mesh gives a section line separating the hemispheres. The last point of this line is identified as the Inion.

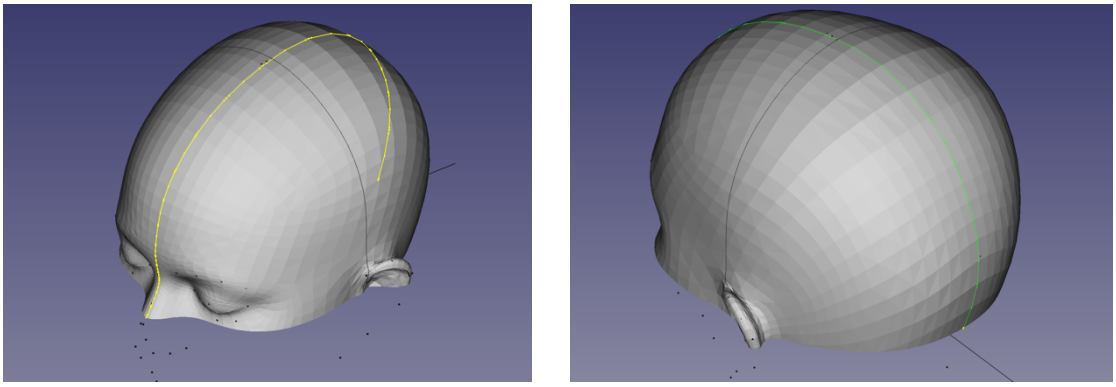

Figure 26 Steps Macro FreeCAD: Nasion-Inion line

Nasion – Inion line and the 11 central points

A cut from Nasion to Inion through the Top is created. Then a path array of 11 points is generated with this wire.

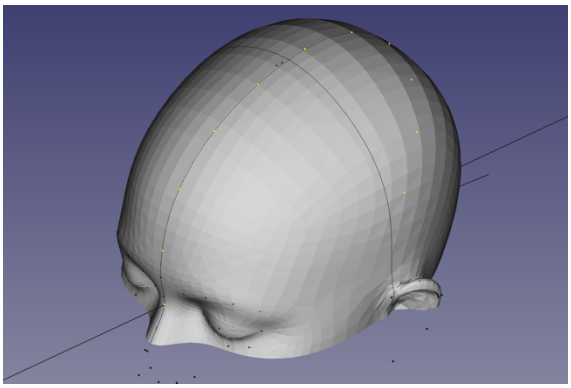

Figure 27 Steps Macro FreeCAD: Nasion-Inion 11 points

Head Circumference plane

A line between Fpz and Oz is created. Also, a vector that lies in the plane Tragus – Cz – Tragus. Then, a Half Point (HP) created at the intersection between this line and this vector. Then a line through this HP and orthogonal to the Nasion – Inion plane is created. With these two lines the Head Circumference (HC) plane is created.

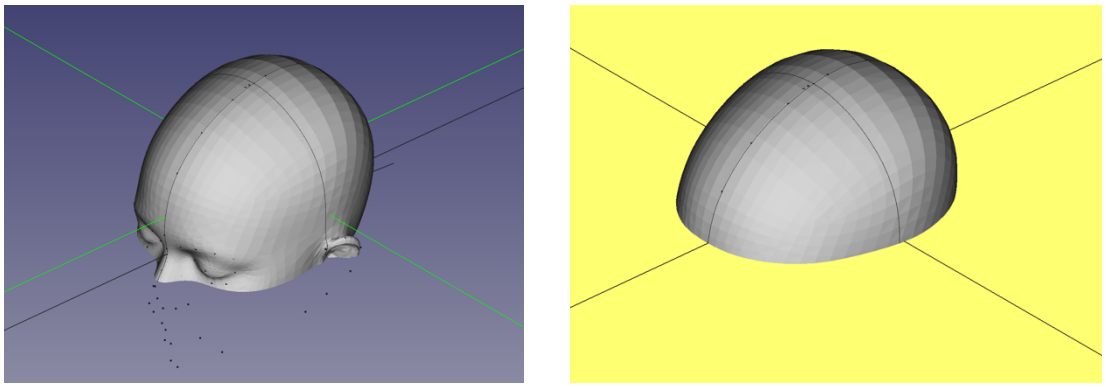

Figure 28 Steps Macro FreeCAD: Head Circumference Plane

With three vertex of this plane a mesh section is created, and the Head Circumference sketch is generated. Then the sketch is turned into a wire.

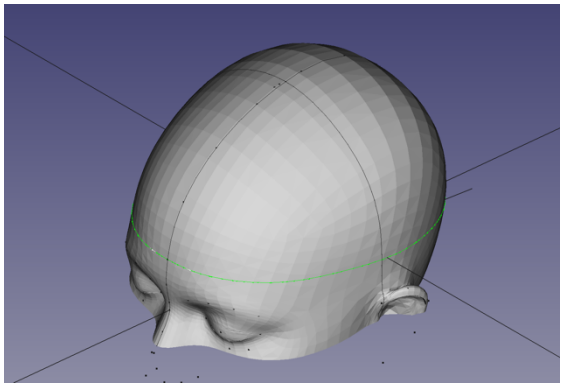

Figure 29 Steps Macro FreeCAD: Head Circumference line

Right and Left Hemispheres and points across HC line

The HC wire is then split where it crosses the Fpz – Oz line, thereby creating the two hemispheres. Then these cuts are turned into wires and to path arrays of 11 points.

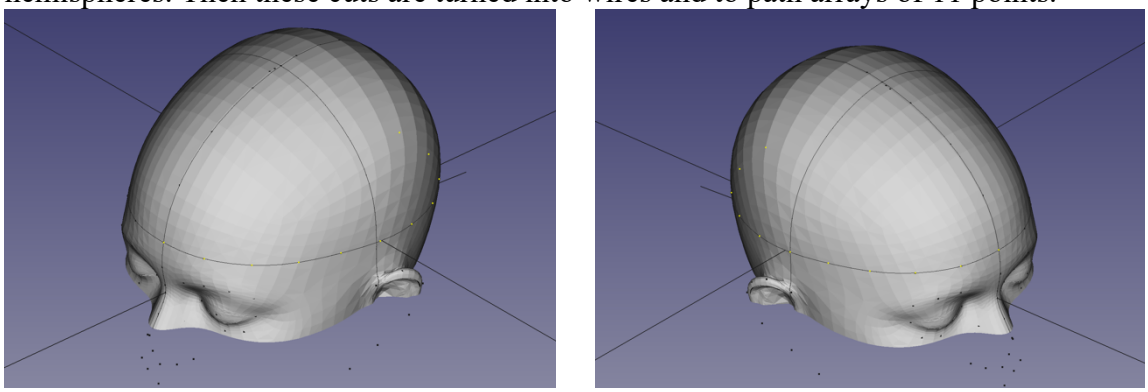

Figure 30 Steps Macro FreeCAD: Right and Left hemisphere points

Auxiliary lines between the points at the left and the right hemispheres are created. Additionally, points are placed at the final vertices of the lines to facilitate the creation of planes latter. Half points in the middle of these lines are also created.

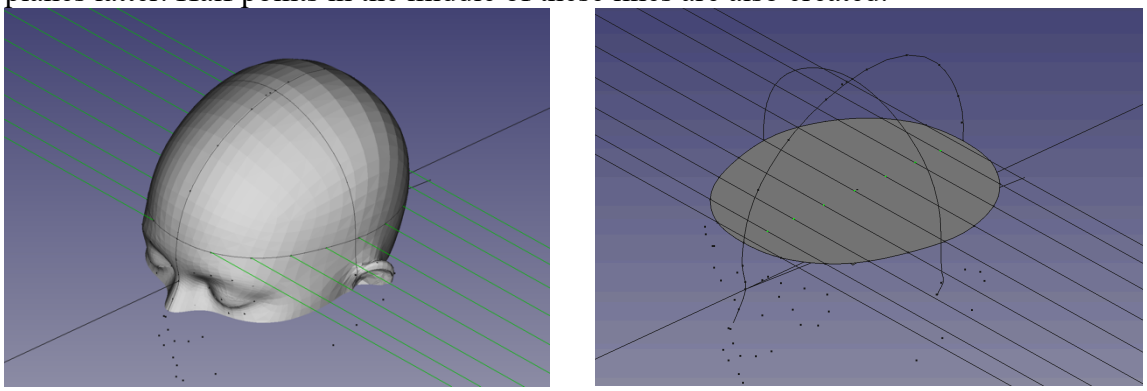

Figure 31 Steps Macro FreeCAD: Auxiliary lines and Half Points

Lines from these HP to their respective points in the Nasion – Inion line are created. Also, points at the end vertices are placed. With the two end points from the previous lines, and this last point lateral cuts at each central point are generated.

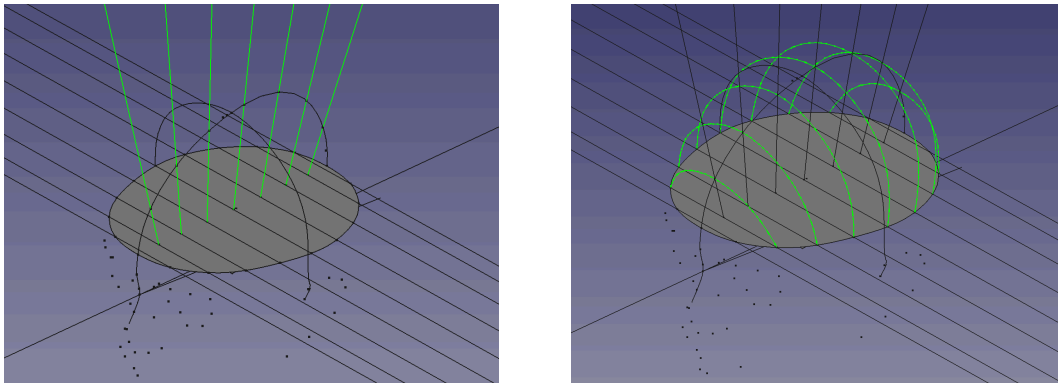

Figure 32 Steps Macro FreeCAD: Lateral Cuts from the points in the Ns-In line to the HC line

International 10/10 System Cranial Points

Each of these cuts is divided into right and left hemispheres. Each wire is turned into a path array (lines AFz and POz with 3 points each, and the rest of the lines with 5 points each), thus obtaining the remaining points of the 10/10 system.

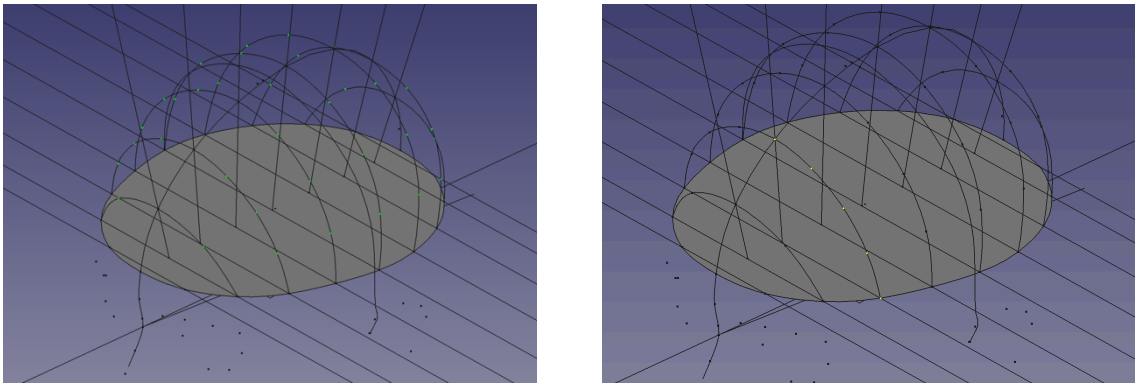

Figure 33 Steps Macro FreeCAD: Localization of all the points in the International 10/20 System

LPA – RPA Line

When a section is made between the mesh and the Tragus – Tragus plane, the resulting cut also includes measurements of the ears. To determine the Tragus-Tragus line measurement, the following steps are taken: the distances from Cz to T7 and Cz to T8 are summed with two straight lines created from T7 to the tragus and from T8 to the tragus.

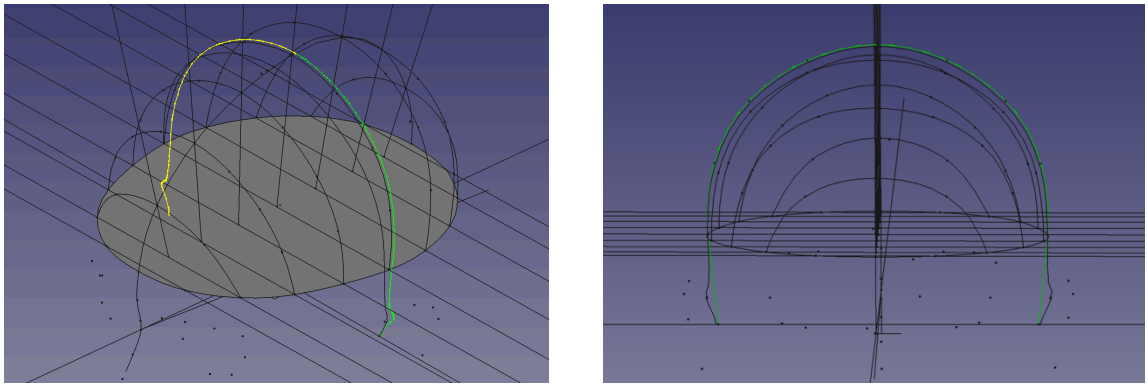

Figure 34 Steps Macro FreeCAD: Tragus-Tragus line

Beam F3 and Adjusted Beam F3 methods

The Beam F3 python code is included in the FreeCAD script. With the measurements of HC, Ns-In line, and Tr-Tr line the calculations to obtain the X, Y and adjusted Y distances are done. Then, a path array of 10.000 points is created in the left hemisphere. By proportionality, the relation of which point correspond to the distance X is calculated and then the point created. Then, is created a cut from the plane that includes this point X, the Cz and the HP at the Cz lines. This cut is turned into another path array of 10.000 points, and Y cm are advanced through this line obtaining the F3 point with the Beam method. The same is done with the adjusted Y (3.5 mm more) for the Adjusted BeamF3 method.

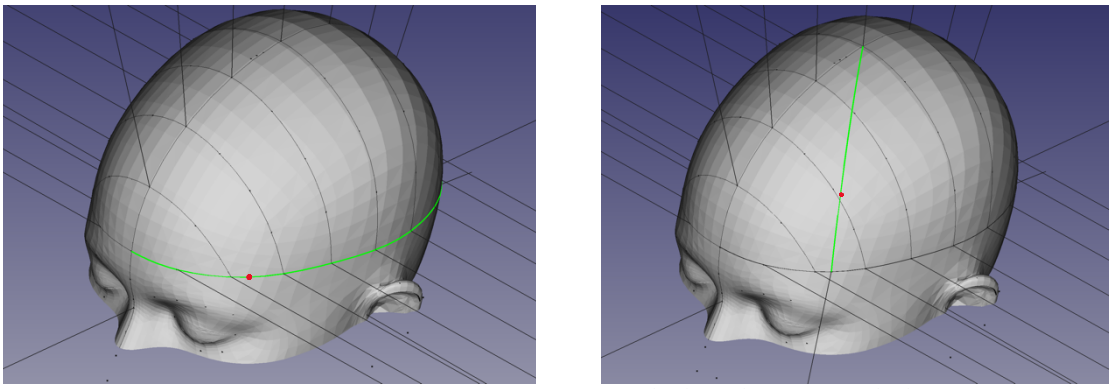

Figure 35 Steps Macro FreeCAD: BeamF3 and Adjusted BeamF3 methods

Updated Scalp Heuristics for localizing the DLPFC

The updated equations are introduced in the code and calculated with the measures HC, Ns-In and LPA-RPA (cm). The distances X and Y for the 4 different locations (LA, RA, LP and RP) are obtained. Then, the same procedure as for the BeamF3 method is done (the path arrays with 10.000 points and the proportional measures). This is repeated for the 4 points to locate. Distances above the scalp are measured from F3 and F4 to each location.

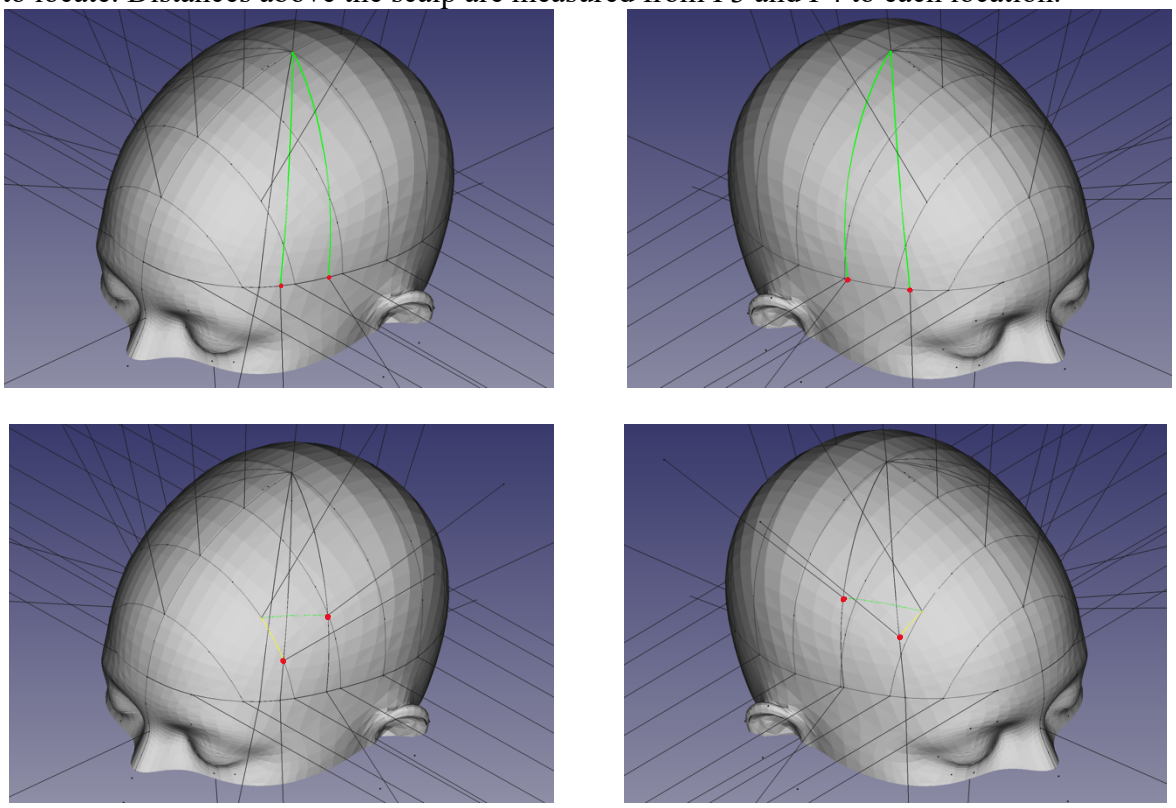

Figure 36 Steps Macro FreeCAD: Updated Scalp Heuristics for localizing the DLPFC

Method 5-7 cm for CP3 and CP4

A cut from Cz to In is created, then a path array of 10.000 points is generated. By using the rule of three, is determined how many points are needed to advance 5 cm along the line. The point Post 5 cm from Cz is founded. A cut from this point to the Tragus is created in each hemisphere. Then another path array of 10.000 points is generated and 7 cm are advanced. Finally, the CP3 and CP4 with the 5-7 cm method are located.

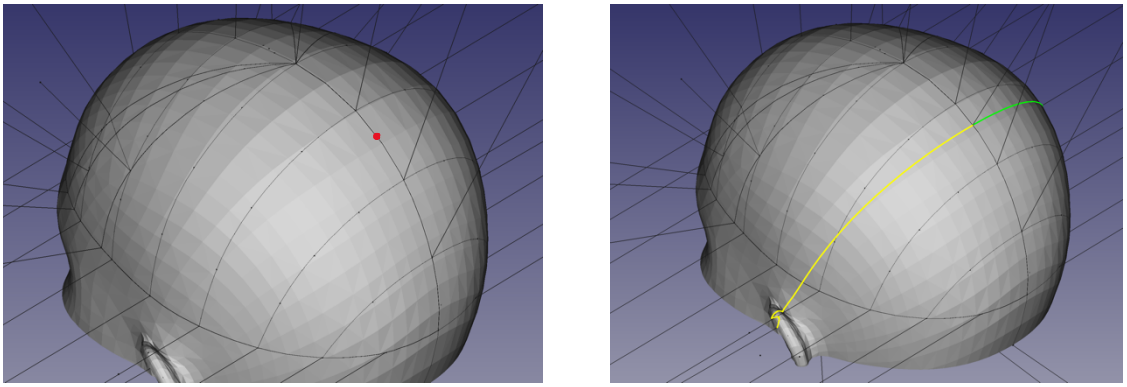

Figure 37 Steps Macro FreeCAD: Method 5-7 cm for localizing CP3 and CP4

Kocher Point

Five different Kocher Points are created, each of them in the two hemispheres (10 total).

Kocher 1 L/R: 11 cm post Nasion and 3 cm lateral.

A line from Ns to FCz is created, then a path array of 10.000 points and by the rule of three the relation of how much points are needed to advance 11 cm is calculated. Then this point is marked. Two extra points with the coordinate X of the Post 11 point are created. A plane and an intersection line are generated. Then a path array of 10000 points for each lateral, and 3 cm are advanced. Then the K1 Left and Right are founded.

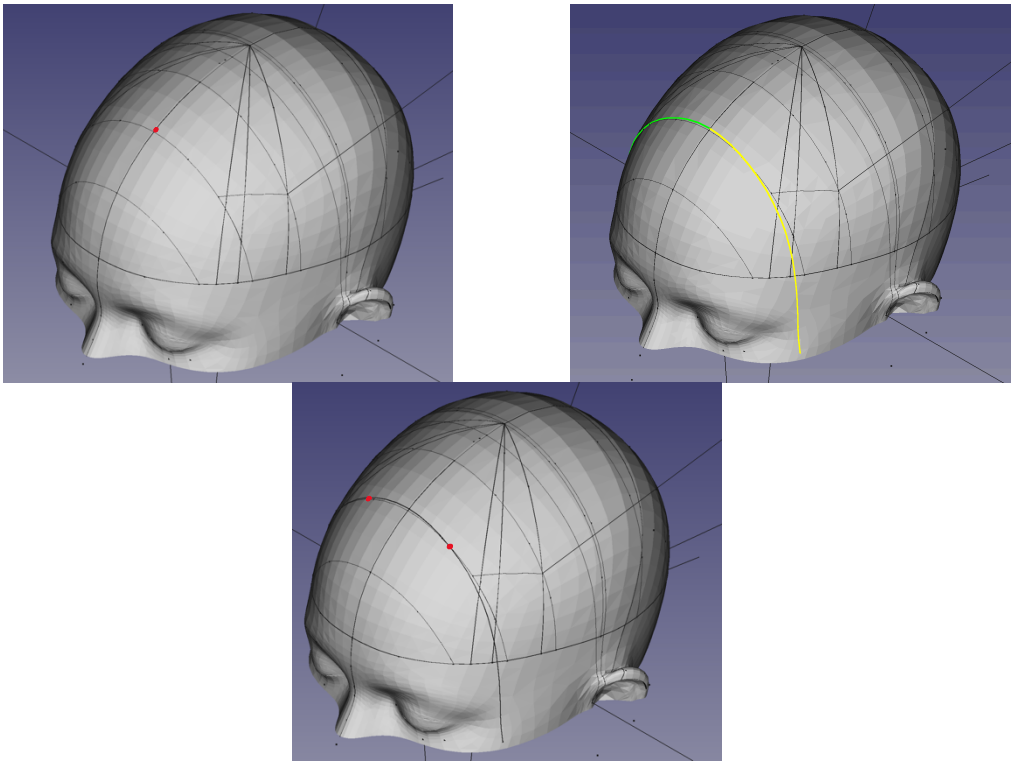

Figure 38 Steps Macro FreeCAD: Kocher 1 - 11 cm post Nasion and 3 cm lateral

Kocher 2 L/R: 11 cm post Nasion and intersection with Mid Pupillary Line
The Mid Pupillary line is created with the landmark Eye Center Infraorbital left and right, and two other points created with the coordinate Y of this point. Using the post 11 cm point and the lateral Path Array, the intersection of the mid pupillary line and the lateral path array is where the Kocher 2 is located.

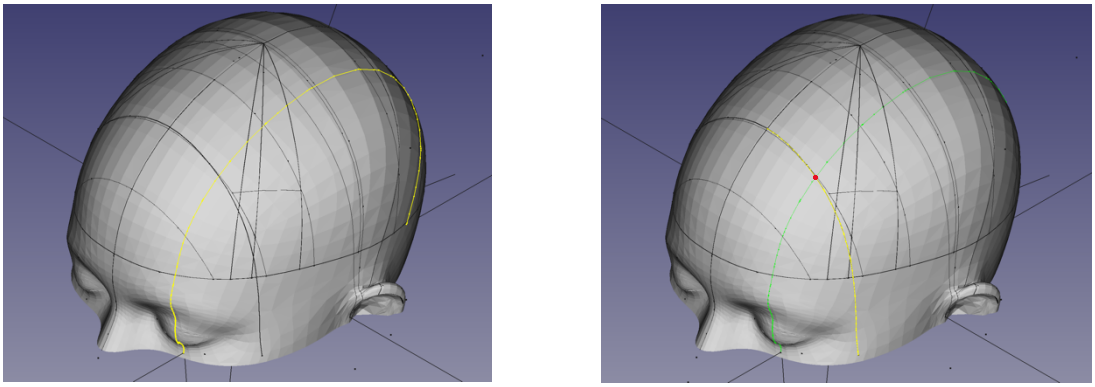

Figure 39 Steps Macro FreeCAD: Kocher 2 - 11 cm post Nasion and intersection with Mid Pupillary line

Kocher 3 L/R: FFC3h and FFC4h of the International 10/5 system.
A Path Array of 3 points is created between Fz and FCz. Two other path arrays of 3 points are created between F7 and FT7, and between F8 and FT8. The middle points of each path array are used to create a plane, then is meshed, a sketch is created, and wires at each hemisphere are created. Path arrays of 9 points are created in each hemisphere and the point number 4 is the FFC3h in the left and the FFC4h in the right.

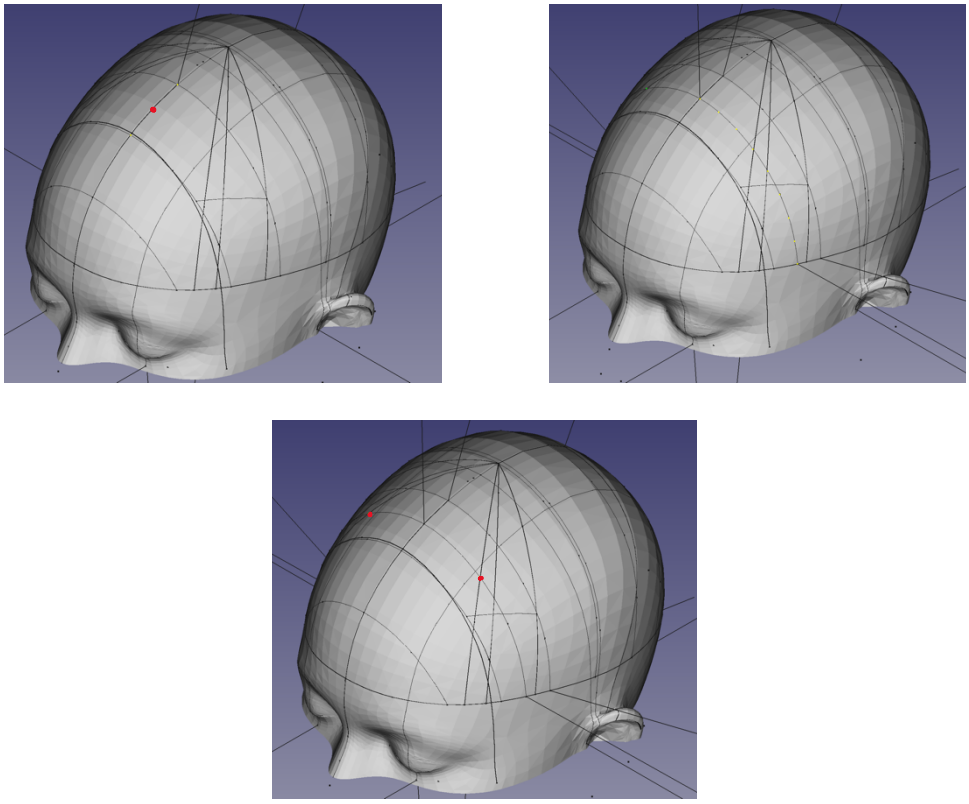

Figure 40 Steps Macro FreeCAD: Kocher 3 – FFC3h and FFC4h

Kocher 4 L/R: Half point between F1 and F3 (L) and between F2 and F4 (R).
A wire from F1 to F3, and a wire from F2 and F4 are created. Then a Path array of 3 points from this wire is generated. The points number 2 of each path array are the Kocher 4 left and right.

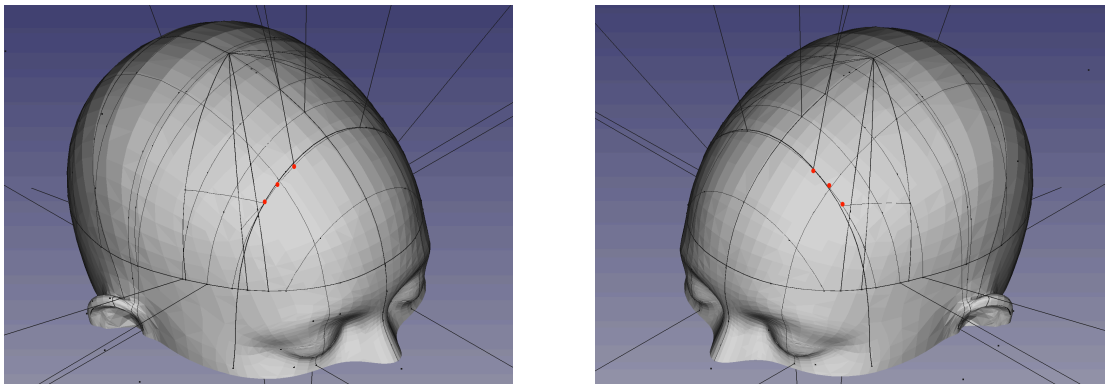

Figure 41 Steps Macro FreeCAD: Kocher 4 – Half point between F1 and F3

Kocher 5 L/R: 2 cm anterior to coronal suture and intersection with Mid Pupillary line.
A path array of 10000 from the head top symmetric point (in the YZ plane) to Fz is created. Then the relation of 2 cm is calculated, and the 2 cm anterior point is located. Two extra points with the coordinate X of the Anterior 2 point are created. A plane and an intersection line are generated. Then this lateral line is intersected with the Mid Pupillary line, locating the Kocher point 5 left and right.

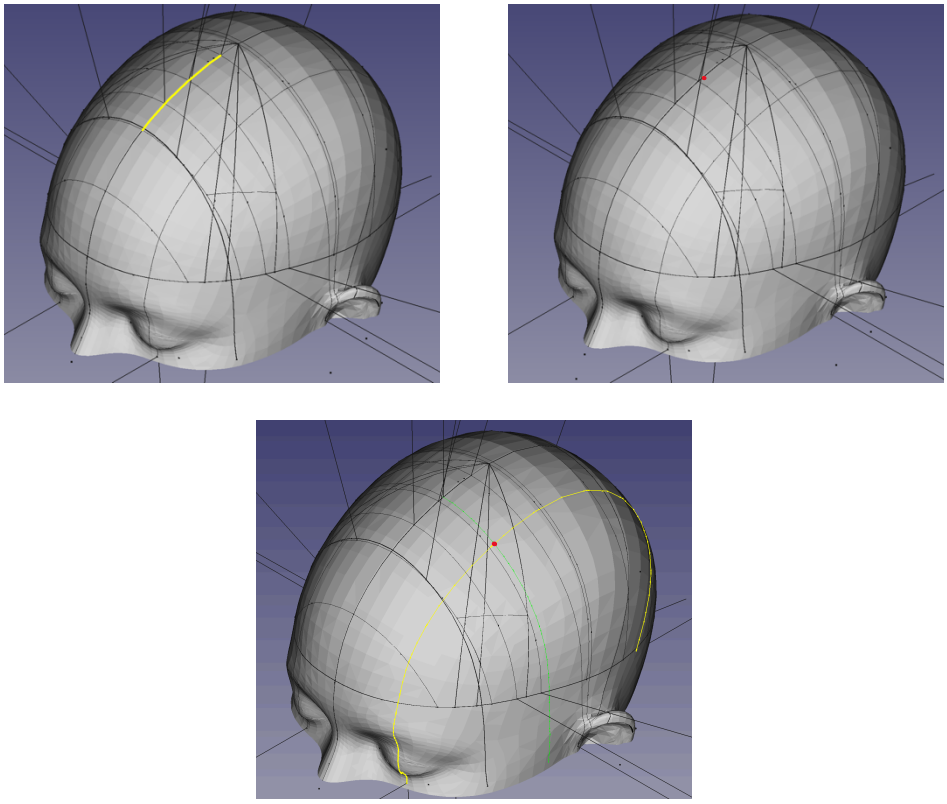

Figure 42 Steps Macro FreeCAD: Kocher 5 – 2 cm anterior to coronal suture and intersection with Mid Pupillary line

EPlacement measures and relations needed

The data in this section has been removed to maintain confidentiality.

Rotation and Translation of the Points

Since the plane that symmetrically cuts through the Nasion, Top, and Inion points is not aligned with the XZ plane (it has a non-zero Y coordinate), with the Nasion having a positive Y coordinate and the Inion a negative one, a calculation of new coordinates in a rotated plane is performed. This involves rotating the original coordinate system to align the plane with the XZ plane, effectively adjusting the Y coordinates to zero.

The procedure involves calculating the normal vector of the Nasion–Top–Inion and comparing it to the normal of the XZ plane. A rotation axis is then determined as the cross product of these normal vectors, and the angle between the two planes is calculated. This rotation is applied to the points, and the rotated points are translated so that the midpoint between the rotated Nasion and Inion aligns with the origin along the Y-axis, ensuring proper alignment and centering for further processing. A function in the code is created to efficiently rotate and transform all necessary points.

Creation and exportation of a Spreadsheet

Finally, all the cranial points coordinates and measurements generated after running all the code are written in a Spreadsheet. It is exported as a CSV file by clicking the Export spreadsheet button.

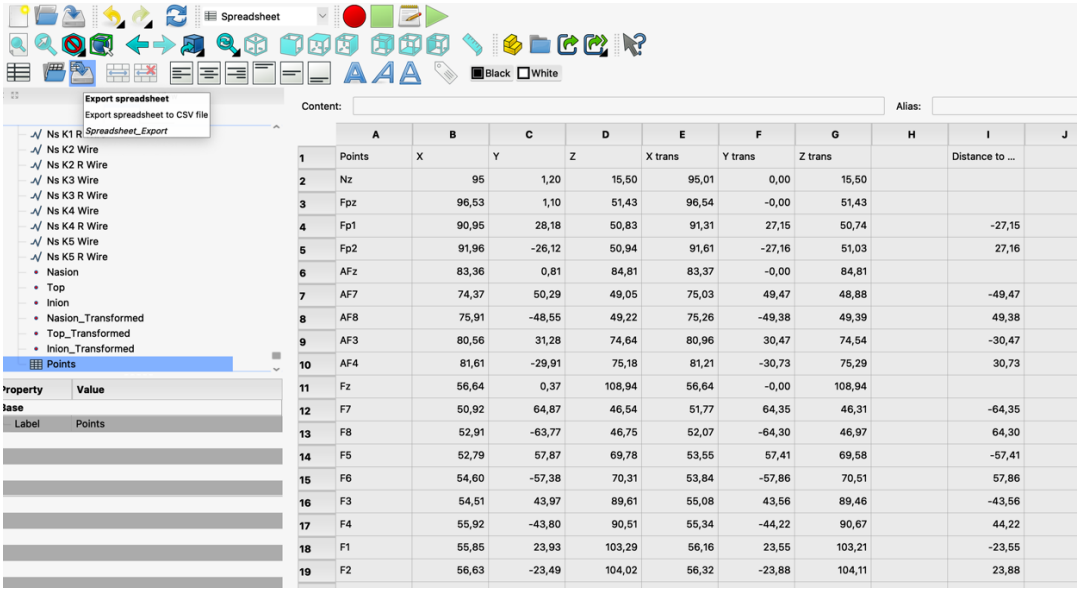

	A	B	C	D	E	F	G	H	I	J
1	Points	X	Y	Z	X trans	Y trans	Z trans		Distance to ...	
2	Nz	95	1,20	15,50	95,01	0,00	15,50			
3	Fpz	96,53	1,10	51,43	96,54	-0,00	51,43			
4	Fp1	90,95	28,18	50,83	91,31	27,15	50,74		-27,15	
5	Fp2	91,96	-26,12	50,94	91,61	-27,16	51,03		27,16	
6	AFz	83,36	0,81	84,81	83,37	-0,00	84,81			
7	AF7	74,37	50,29	49,05	75,03	49,47	48,88		-49,47	
8	AF8	75,91	-48,55	49,22	75,26	-49,38	49,39		49,38	
9	AF3	80,56	31,28	74,64	80,96	30,47	74,54		-30,47	
10	AF4	81,61	-29,91	75,18	81,21	-30,73	75,29		30,73	
11	Fz	56,64	0,37	108,94	56,64	-0,00	108,94			
12	F7	50,92	64,87	46,54	51,77	64,35	46,31		-64,35	
13	F8	52,91	-63,77	46,75	52,07	-64,30	46,97		64,30	
14	F5	52,79	57,87	69,78	53,55	57,41	69,58		-57,41	
15	F6	54,60	-57,38	70,31	53,84	-57,86	70,51		57,86	
16	F3	54,51	43,97	89,61	55,08	43,56	89,46		-43,56	
17	F4	55,92	-43,80	90,51	55,34	-44,22	90,67		44,22	
18	F1	55,85	23,93	103,29	56,16	23,55	103,21		-23,55	
19	F2	56,63	-23,49	104,02	56,32	-23,88	104,11		23,88	

Figure 43 Steps Macro FreeCAD: Final Spreadsheet with all the points and measures

2.4 Statistical analysis models

After obtaining the 250 CSV files, a Python script is used to generate a consolidated database. This database includes the three study variables: Ns-In, LPA-RPA, and HC (head circumference), along with the variables to be analyzed. The variables analyzed for their dependence on the 3 study variables are: Distance F3-BeamF3, Distance F3-BeamF3Adj, LP-F3 scalp distance, LA-F3 scalp distance, RP-F4 scalp distance, RA-F4 scalp distance, %Nasion, %Ns inclined, and %Tragus for each of the required points.

2.4.1 Multiple Linear Regression

The initial approach was to perform a **linear regression**, it is a statistical modeling technique used to describe a continuous response variable as a function of one or more predictor variables [37]. Linear regression methods enable the creation of a linear model that characterizes the relationship between a dependent variable Y and one or more independent variables Xi (predictors). When there is more than one X predictor, it is referred to as **Multiple Linear Regression**. The equation for this model is:

$$Y = \beta_0 + \beta_1 X_1 + \beta_2 X_2 + \epsilon \qquad \text{(Eq. 10)}$$

where:

- Y is the dependent variable (response).
- X1, X2, …, Xp are the independent variables (predictors).
- β0 is the intercept.
- β1, β2, …, βp are the coefficients for each predictor.
- ϵ is the error term.

The Multiple Linear Regression assumes that the predictor variables X1, X2, ..., Xp, are linearly independent. In the case that two variables are highly correlated the presence of multicollinearity is indicated. **Multicollinearity** occurs when there are strong linear relationships between two or more independent variables in a multiple linear regression model [38]. This can lead to unreliable estimates of regression coefficients and difficulties in interpreting the effects of predictors on the response variable. Therefore, it is important to evaluate if the variance increase is caused by multicollinearity, to understand its impact on the regression model's reliability.

2.4.2 Variance Inflator Factor (VIF)

The Variance Inflation Factor (VIF) is a measure used to quantify the level of multicollinearity in a regression analysis [39]. It estimates how much the variance of a regression coefficient is inflated due to multicollinearity. This is the equation, being R^2 the coefficient of determination of the regression equation.

$$VIF_i = \frac{1}{1 - R_i^2} \qquad \text{(Eq. 11)}$$

The higher the VIF, the higher the possibility that multicollinearity exists, and further research is required. When VIF is higher than 10, there is significant multicollinearity that needs to be corrected [40].

3 Results and Discussion

3.1 Obtained Measurements of HC, Ns-In, and LPA-RPA

Firstly, from the database obtained and explained in the previous section, the anthropometric measurements of the 250 heads are analyzed. The measurements of the three key study variables Head Circumference (HC), Nasion-Inion (Ns-In) and Tragus-Tragus (LPA-RPA), including the mean, the standard deviation (SD), the minimum and the maximum are summarized in the following histogram and table. Also, there is a fourth column which represents de difference between the Ns-In distance and the LPA-RPA distance. There are 71 heads with smaller Ns-In line, and 179 with smaller LPA-RPA line. But from this 179, 36 have a difference of less than 10 mm.

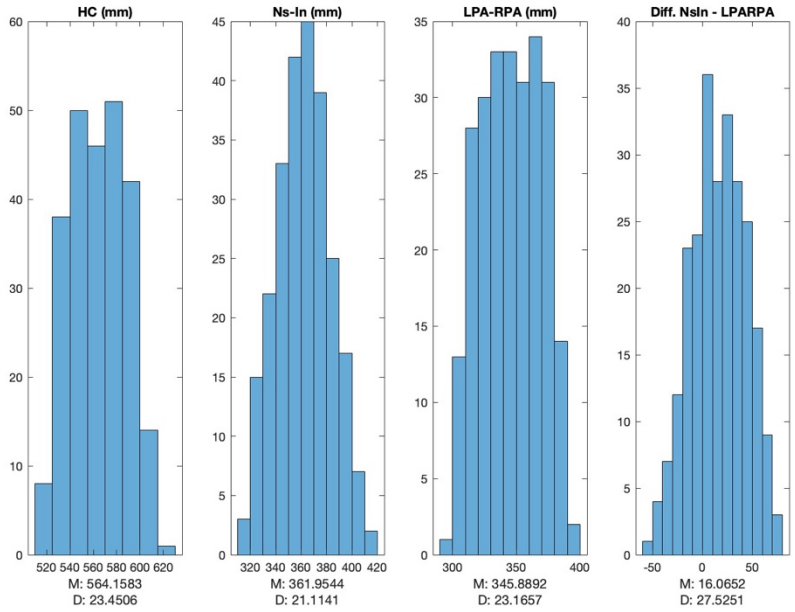

Figure 44 Histogram of obtained measurements: HC, Ns-In, LPA-RPA and difference NsIn - LPARPA (mm)

	Mean	SD	Minimum	Maximum
HC (mm)	564.2	23.4	514.4	617
Ns-In (mm)	361.9	21.1	313.9	413.3
LPA-RPA (mm)	345.8	23.2	298.3	390.9

Table 7 Results of obtained HC, Ns-In and LPA-RPA (mm) for a sample of 250 heads

These results indicate that the heads analyzed comprehend most of the population because the minimum range is achieved, and the maximum values are slightly under the target scalp-based measurements obtained by Mir-Moghtadaei et al. (2015) [31] mentioned in "Methods and Materials". Tables separated by gender are also represented.

FEMALE	Mean	SD	Minimum	Maximum
HC (mm)	559.1	22.52	514.4	606.3
Ns-In (mm)	363.4	21.19	314.1	413.3
LPA-RPA (mm)	345.9	23.14	301.5	390.9

Table 8 Results of obtained HC, Ns-In and LPA-RPA (mm) for a sample of 125 female heads

MALE	Mean	SD	Minimum	Maximum
HC (mm)	569.2	23.35	525.1	617
Ns-In (mm)	360.4	21.01	313.9	411
LPA-RPA (mm)	345.8	23.27	298.3	390.6

Table 9 Results of obtained HC, Ns-In and LPA-RPA (mm) for a sample of 125 male heads

3.2 Analysis of T-Test Results and Justification for Separate Analysis by Gender

As the previous results show a difference between the female and male head models, a t-test is performed to evaluate if there is a significance difference between them, and therefore the need to perform the analyses separately.

	HC	Ns-In	LPA-RPA
H value	1	1	0
p-value	2.85E-90	1.38E-17	0.8168

Table 10 Results of the t-test analysis supporting the justification for separate analysis by gender

Although the p-value for the LPA-RPA t-test is high and means no significant difference, the low p-values for the HC and Ns-In t-tests indicate statistically significant difference between male and female head models. For this reason, separated analysis based on gender could lead to more accurate results, as these observed differences in anthropometric measurements could potentially influence later analyses.

3.3 Pearson Correlation, Multicollinearity and VIF Analysis

Multicollinearity occurs when there are strong linear relationships between two or more independent variables in a multiple linear regression model [38]. This can lead to difficulties in accurately estimating and interpreting the regression coefficients. To assess multicollinearity, it is common to examine the Pearson correlation coefficients between the independent variables.

Pearson Correlation Female and Male

Female	HC	Ns-In	Tr-Tr
HC	1.000	0.8748	0.4303
Ns-In	0.8748	1.000	0.2854
Tr-Tr	0.4303	0.2854	1.000

Male	HC	Ns-In	Tr-Tr
HC	1.000	0.8669	0.3673
Ns-In	0.8669	1.000	0.1752
Tr-Tr	0.3673	0.1752	1.000

Table 11 Results of Pearson Correlation Female (left) and Male (right)

A high correlation, such as that observed between HC and Ns-In, indicates potential multicollinearity. The Variance Inflation Factor (VIF) measures how much the variance of a regression coefficient is inflated due to multicollinearity [40] . If the VIF for a variable exceeds a threshold set at 10, it indicates severe multicollinearity, which could negatively impact the model's reliability. However, since the VIF values are below 10 in this case, it suggests that multicollinearity is not severe, and the multiple linear regression can be conducted without significant concerns.

VIFs Female and Male of each independent variable (HC, Ns-In and LPA-RPA)

	Female	Male
HC	5.0184	4.9859
Ns-In	4.4517	4.4500
Tr-Tr	1.2828	1.2779

Table 12 Results of VIFs Female and Male

3.4 Analysis of different Heuristic Methods for Cranial Point Localization

3.4.1 Analysis of Beam F3 method

For these analyses the Euclidean distance between F3 in the International 10/20 System and the F3 located with Beam F3 method is studied.

$$d = \sqrt{(x_1 - x_0)^2 + (y_1 - y_0)^2 + (z_1 - z_0)^2} \qquad \text{(Eq. 12)}$$

The data in this section has been removed to maintain confidentiality.

3.4.2 Analysis of Adjusted Beam F3 method

The data in this section has been removed to maintain confidentiality.

3.4.3 Analysis of Updated Scalp Heuristics for localizing DLPFC

The data in this section has been removed to maintain confidentiality.

3.4.4 Analysis of Method 5-7 cm for CP3 and CP4

The data in this section has been removed to maintain confidentiality.

3.4.5 Analysis of Kocher's Point Localization

The data in this section has been removed to maintain confidentiality.

3.5 EPlacement Percentages Results

3.5.1 EPlacement Percentages: F3 and F4

3.5.2 EPlacement Percentages: CP3 and CP4

3.5.3 EPlacement Percentages: P3 and P4

3.5.4 EPlacement Percentages: O1 and O1

3.5.5 EPlacement Percentages: Kocher Point

The data in these sections have been removed to maintain confidentiality.

4 Conclusion

This study was conducted using head models obtained from the HumanShape website, with a sample of 250 heads, consisting of 125 female and 125 male models. The parameters of the HumanShape models were adjusted to achieve realistic measurements of Head Circumference (HC), Nasion-Inion line (Ns-In) and Tragus-Tragus line (LPA-RPA) that accurately represent the population. Head measurements that fall within the realistic ranges were successfully generated. A greater number of heads were obtained with the Ns-In line higher than the LPA-RPA line.

A Python script in the FreeCAD software was developed to automate the process of cranial point localization, eliminating the need for manual intervention. This automation significantly streamlined the process, enabling the efficient localization of cranial points across all 250 head models. The tool developed in this study proved to be highly effective and could be used in future research to further refine and evaluate cranial point localization methods.

In this study, a direct comparison was made between cranial point localization using the International 10/20 System and different heuristic methods. A statistical analysis was performed to evaluate the differences between these methods. The analysis was conducted separately for female and male head models, as significant differences were observed in the cranial measurements based on gender.

Beam F3 and Adjusted BeamF3 method:

- The data in this section has been removed to maintain confidentiality.

Updated scalp heuristics for localizing DLPFC:

- The data in this section has been removed to maintain confidentiality.

Method 5-7cm for localizing CP3 and CP4:

- The data in this section has been removed to maintain confidentiality.

Heuristic method for Kocher's Point Localization:

- The data in this section has been removed to maintain confidentiality.

EPlacement:
The results from the EPlacement percentages show that for different head shapes, the same percentage can be used to calculate the distance from Nasion to the targeted 10/20 system point along the inclined Ns-In line, and the other percentage can be used to calculate the distance from Cz to C3' or C4' along the LPA-RPA line. The mean value of each percentage can be used reliably due to the small standard deviation (SD), indicating minimal variability.

- The data in this section has been removed to maintain confidentiality.

In summary, this study demonstrates that while heuristic methods offer a practical and quickly way to locate the International 10/20 System cranial points, significant discrepancies can arise depending on individual head morphology. The findings highlight that HC, Ns-In and LPA-RPA measurements are statistically significant factors influencing these differences. The EPlacement device shows promise in standardizing the process, with consistent percentages yielding reliable results across different head shapes.

5 References

[1] "Brain Anatomy and How the Brain Works | Johns Hopkins Medicine." Accessed: Jul. 09, 2024. [Online]. Available: https://www.hopkinsmedicine.org/health/conditions-and-diseases/anatomy-of-the-brain

[2] "Entendiendo al cerebro: potenciales de acción y sinapsis Dacer centro de neurorrehabilitación y daño cerebral." Accessed: Aug. 24, 2024. [Online]. Available: https://www.dacer.org/entendiendo-al-cerebro-potenciales-de-accion-y-sinapsis/

[3] "Action Potential Basics - Neurology - Medbullets Step 1." Accessed: Aug. 24, 2024. [Online]. Available: https://step1.medbullets.com/neurology/113052/action-potential-basics

[4] "Brain Anatomy | Mayfield Brain & Spine Cincinnati, Ohio." Accessed: Jul. 09, 2024. [Online]. Available: https://mayfieldclinic.com/pe-anatbrain.htm

[5] P. Chauhan, A. Rathawa, K. Jethwa, and S. Mehra, "The Anatomy of the Cerebral Cortex," *Cerebral Ischemia*, pp. 1–16, Nov. 2021, doi: 10.36255/EXONPUBLICATIONS.CEREBRALISCHEMIA.2021.CEREBRALCORTEX.

[6] "Brain Anatomy and How the Brain Works | Johns Hopkins Medicine." Accessed: Jul. 09, 2024. [Online]. Available: https://www.hopkinsmedicine.org/health/conditions-and-diseases/anatomy-of-the-brain

[7] G. Morales and J. Artieda, "La neurofisiología clínica: pasado, presente y futuro," *An Sist Sanit Navar*, vol. 32, pp. 5–8, 2009, Accessed: Aug. 05, 2024. [Online]. Available: https://scielo.isciii.es/scielo.php?script=sci_arttext&pid=S1137-66272009000600001&lng=es&nrm=iso&tlng=es

[8] "L'Electroencefalografia (EEG) i Potencials Evocats | Centre Mèdic Teknon." Accessed: Aug. 05, 2024. [Online]. Available: https://www.teknon.es/ca/proves-diagnostiques/electrofisiologia/l-electroencefalografia-eeg-i-potencials-evocats

[9] "Polysomnography (sleep study) - Mayo Clinic." Accessed: Aug. 05, 2024. [Online]. Available: https://www.mayoclinic.org/tests-procedures/polysomnography/about/pac-20394877

[10] M. Gupta, S. E. Taylor, R. A. O'Brien, W. R. Taylor, and L. Hein, "Intraoperative Neurophysiological Monitoring," *Minimally Invasive Spine Surgery: Surgical Techniques and Disease Management*, pp. 69–81, Jul. 2023, doi: 10.1007/978-3-030-19007-1_7.

[11] F. Tergau and B. J. Steinhoff, "Repetitive Transcranial Magnetic Stimulation," *Textbook of Epilepsy Surgery*, pp. 1208–1219, Mar. 2023, doi: 10.2165/00023210-200317060-00002.

[12] N. T. Trapp *et al.*, "Reliability of targeting methods in TMS for depression: Beam F3 vs. 5.5 cm," May 01, 2020, *Elsevier Inc.* doi: 10.1016/j.brs.2020.01.010.

[13] "Ventriculostomy: What It Is, Purpose, Procedure & Risks." Accessed: Aug. 09, 2024. [Online]. Available: https://my.clevelandclinic.org/health/procedures/ventriculostomy

[14] D. A. . Taylor, S. P. . Sherry, and R. F. . Sing, "Interventional critical care : a manual for advanced care practitioners," p. 467, 2016.

[15] V. Jurcak, D. Tsuzuki, and I. Dan, "10/20, 10/10, and 10/5 systems revisited: Their validity as relative head-surface-based positioning systems," *Neuroimage*, vol. 34, no. 4, pp. 1600–1611, Feb. 2007, doi: 10.1016/j.neuroimage.2006.09.024.

[16] R. Shriram, M. Sundhararajan, M. Sundhararajan, and N. Daimiwal, "EEG Based Cognitive Workload Assessment for Maximum Efficiency," SICETE. [Online]. Available: www.iosrjournals.org

[17] H. Dong, A. Supratak, W. Pan, C. Wu, P. M. Matthews, and Y. Guo, "Mixed Neural Network Approach for Temporal Sleep Stage Classification," *IEEE Transactions on Neural Systems and Rehabilitation Engineering*, vol. 26, no. 2, pp. 324–333, Feb. 2018, doi: 10.1109/TNSRE.2017.2733220.

[18] A. Fabregat-Sanjuan, R. Pàmies-Vilà, and V. Pascual-Rubio, "Evaluation of the Beam-F3 method for locating the F3 position from the 10–20 international system," Jul. 01, 2022, *Elsevier Inc.* doi: 10.1016/j.brs.2022.07.002.

[19] "F3 Measurement System." Accessed: Aug. 05, 2024. [Online]. Available: https://clinicalresearcher.org/F3/calculate.php

[20] W. Beam, J. J. Borckardt, S. T. Reeves, and M. S. George, "An efficient and accurate new method for locating the F3 position for prefrontal TMS applications," *Brain Stimul*, vol. 2, no. 1, p. 50, Jan. 2009, doi: 10.1016/J.BRS.2008.09.006.

[21] A. Mir-Moghtadaei *et al.*, "Concordance between BeamF3 and MRI-neuronavigated target sites for repetitive transcranial magnetic stimulation of the left dorsolateral prefrontal cortex," *Brain Stimul*, vol. 8, no. 5, pp. 965–973, Sep. 2015, doi: 10.1016/j.brs.2015.05.008.

[22] A. Mir-Moghtadaei *et al.*, "Updated scalp heuristics for localizing the dorsolateral prefrontal cortex based on convergent evidence of lesion and brain stimulation studies in depression," *Brain Stimul*, vol. 15, no. 2, pp. 291–295, Mar. 2022, doi: 10.1016/j.brs.2022.01.013.

[23] C. Y. C. Chau *et al.*, “The Evolution of the Role of External Ventricular Drainage in Traumatic Brain Injury,” *Journal of Clinical Medicine 2019, Vol. 8, Page 1422*, vol. 8, no. 9, p. 1422, Sep. 2019, doi: 10.3390/JCM8091422.

[24] S. Munakomi and J. M. Das, “Ventriculostomy,” *StatPearls*, Aug. 2023, Accessed: Aug. 09, 2024. [Online]. Available: https://www.ncbi.nlm.nih.gov/books/NBK545317/

[25] A. Fabregat-Sanjuan, R. Pàmies-Vilà, A. Rigo-Vidal, and V. Pascual-Rubio, “Comparison of electrode position marking procedures on the cranial surface,” *Brain Behav*, vol. 13, no. 10, Oct. 2023, doi: 10.1002/brb3.3187.

[26] A. , & P. R. V. Fabregat Sanjuan, “Method and system for guiding electrode placement on the scalp (EP21382429). European Patent Office.,” 2021

[27] A. Fabregat-Sanjuan, R. Pàmies-Vilà, A. Rigo-Vidal, and V. Pascual-Rubio, “Comparison of electrode position marking procedures on the cranial surface,” *Brain Behav*, vol. 13, no. 10, Oct. 2023, doi: 10.1002/BRB3.3187.

[28] “UMTRI HumanShape™: 3D Human Shapes.” Accessed: Jun. 10, 2024. [Online]. Available: https://humanshape.org/

[29] B.-K. D. Park, B. D. Corner, J. A. Hudson, J. Whitestone, C. R. Mullenger, and M. P. Reed, “A Three-Dimensional Parametric Adult Head Model with Representation of Scalp Shape Variability Under Hair.” [Online]. Available: http://artec3d.com

[30] K. P. Wankhede, V. P. Anjankar, M. P. Parchand, N. Y. Kamdi, and S. T. Patil, “ESTIMATION OF STATURE FROM HEAD LENGTH & HEAD BREADTH IN CENTRAL INDIAN POPULATION: AN ANTHROPOMETRIC STUDY,” *International Journal of Anatomy and Research*, vol. 3, no. 1, pp. 954–957, Mar. 2015, doi: 10.16965/ijar.2015.125.

[31] A. Mir-Moghtadaei *et al.*, “Concordance between BeamF3 and MRI-neuronavigated target sites for repetitive transcranial magnetic stimulation of the left dorsolateral prefrontal cortex,” *Brain Stimul*, vol. 8, no. 5, pp. 965–973, Sep. 2015, doi: 10.1016/j.brs.2015.05.008.

[32] “Getting started - FreeCAD Documentation.” Accessed: Jun. 10, 2024. [Online]. Available: https://wiki.freecad.org/Getting_started#Exploring_the_interface

[33] “Macros - FreeCAD Documentation.” Accessed: Jun. 10, 2024. [Online]. Available: https://wiki.freecad.org/Macros

[34] “Mesh - FreeCAD Documentation.” Accessed: Jun. 10, 2024. [Online]. Available: https://wiki.freecad.org/Mesh

[35] “Draft Workbench - FreeCAD Documentation.” Accessed: Jun. 10, 2024. [Online]. Available: https://wiki.freecad.org/Draft_Workbench

[36] “PartDesign Workbench - FreeCAD Documentation.” Accessed: Jun. 10, 2024. [Online]. Available: https://wiki.freecad.org/PartDesign_Workbench

[37] “Introducción a la regresión lineal - MATLAB & Simulink.” Accessed: Jun. 10, 2024. [Online]. Available: https://es.mathworks.com/discovery/linear-regression.html

[38] S. Streukens and S. Leroi-Werelds, “Multicollinearity: An Overview and Introduction of Ridge PLS-SEM Estimation,” *Partial Least Squares Path Modeling*, pp. 183–207, 2023, doi: 10.1007/978-3-031-37772-3_7.

[39] “Variance Inflation Factor (VIF).” Accessed: Aug. 16, 2024. [Online]. Available: https://www.investopedia.com/terms/v/variance-inflation-factor.asp

[40] M. H. Kutner, M. H. Kutner, C. J. Nachtsheim, and J. Neter, *Applied Linear Regression Models*, 4th ed. McGraw-Hill Irwin, 2004. Accessed: Aug. 15, 2024. [Online]. Available: https://archive.org/details/appliedlinearreg0000kutn

ANNEX

Annex 1 – Procedure to obtain the Cranial Points in FreeCAD manually

The initial step involves executing a line of code to import the head model as a Mesh object and reading the landmark file to draw each point. Then, the head is cut with a plane placed at the Z of the z coordinate of the Inion got by the ID.

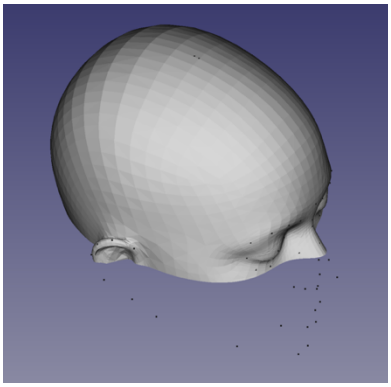

Symmetric Top Point

The YZ reference plane is created, passing through both Tragus. Then, in the Part workbench, an exact plane is generated. Finally, using this latter plane and the Head Mesh, a section is created at their intersection. This section is converted to a Sketch and cut from Tragus to Tragus. Then a Path Array of 3 points is created, and the middle point is the new Head Top point.

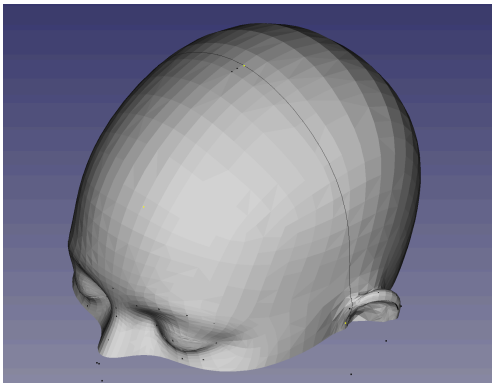

Plane Right/Left Hemisphere

In the Part Design workbench, the points Nasion (Nose Sellion Center), Origin (0,0,0), and Top are converted from Draft points to Datum points. Using these three points, a plane is created. Then, in the Part workbench, an exact plane is generated. Finally, using this latter plane and the Head Mesh, a section is created at their intersection.

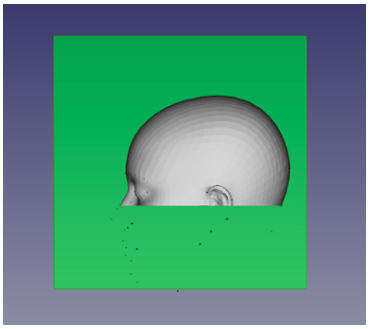

Nasion-Inion Line

In the Draft workbench, the section generated is converted to sketch. In the Sketcher the lines from the section that are before the Nasion are cut. The final sketch is converted to a Wire and after to a B-Spline. With a draft point and the B-Spline a PathArray with 11 points is generated, being this the Nasion-Inion line with the Nz to Iz points, being the last of these points the Inion.

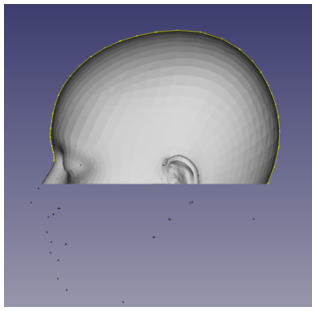

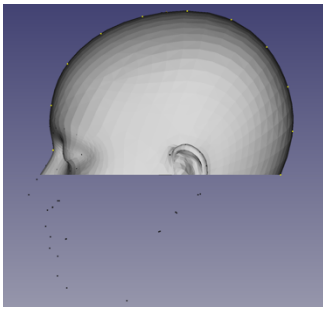

Head Circumference Line

In the Part Design workbench, a line between the points Fpz and Oz, and a line between the origin and Cz are created. In the intersection of these lines a half-point HP is created. Now, a line coincident with HP and orthogonal with the plane XZ is created. With this latter line and the Fpz-Oz line, the Head Circumference Plane is created. Then, in the Part workbench, an exact plane is generated. Finally, using this latter plane and the Head Mesh, a section is created at their intersection. The HC section is converted to sketch.

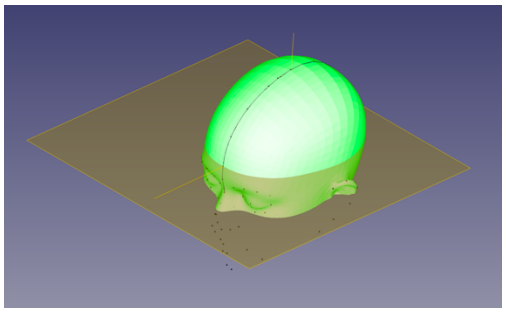

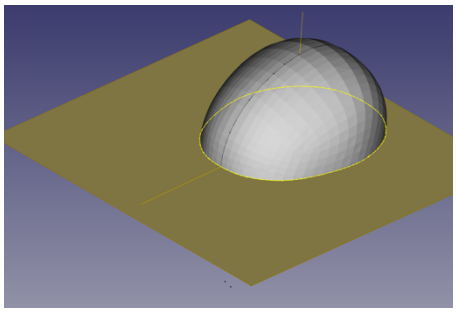

Left and Right Hemisphere points

The right and left hemisphere wires are obtained by cutting the HC sketch in two equal parts. Then the sketches are converted to Wire and B-Spline in the Draft workbench, and after converted to Path Arrays of 11 points each of them. The points at the left are: Fpz, Fp1, AF7, F7, FT7, T7, TP7, P7, PO7, O1 and Oz. The points at the right are: Fpz, Fp2, AF8, F8, FT8, T8, TP8, P8, PO8, O2 and Oz.

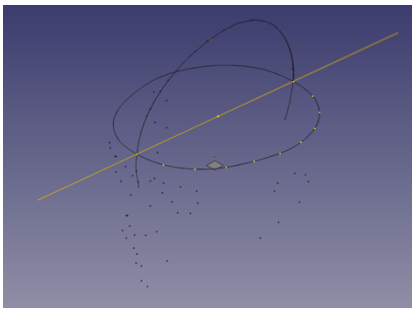

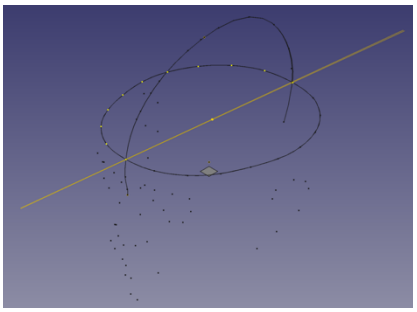

Planes and cuts in each plane of points

In each case the procedure is: create a plane with 3 points in the Part Design workbench (two points in the hemispheres and the respective point in the Ns-In line), replicate the plane in the Part workbench, create a section in the intersection between the head and the plane in the Mesh workbench and cut the needed line of the section in the Sketcher. This needs to be done 7 times obtaining the following lines:

- Line AFz: from AF7 to AF8 passing through AFz.
- Line FZ: from F7 to F8 passing through FZ.
- Line FCz: from FT7 to FT8 passing through FCz.
- Line Cz: from T7 to T8 passing through Cz.
- Line CPz: from TP7 to TP8 passing through CPz.
- Line Pz: from P7 to P8 passing through Pz.
- Line POz: from PO7 to PO8 passing through POz.

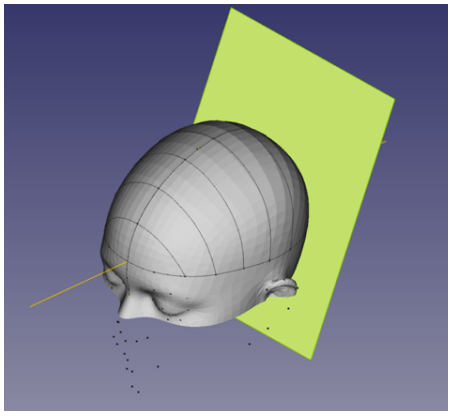

Path Arrays with the remaining points of the International 10/20 system

The sketch lines obtained in the previous step are duplicated and cut into two exact parts: one for the Left hemisphere and the other for the Right. This method ensures that more symmetric points are obtained by working separately on the two hemispheres. The Right and Left sketches of the lines are converted to wires, then to B-splines, and finally to path arrays (lines AFZ and POz with 3 points each, and the rest of the lines with 5 points each), thus obtaining the remaining points of the 10/20 system.

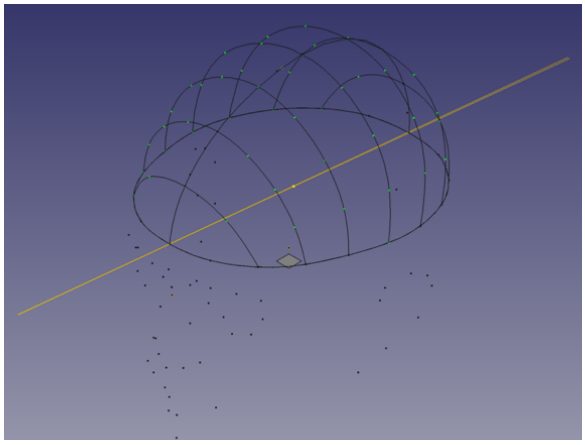

LPA-RPA line

To obtain the measurement of the LPA-RPA line, the following steps are taken: the sum of the wires Cz left and Cz right, plus the cuts from T7 to Tragus and T8 to Tragus. This method is used because the head models include ears, and creating the section directly would result in the line passing over the ear, leading to inaccurate results.

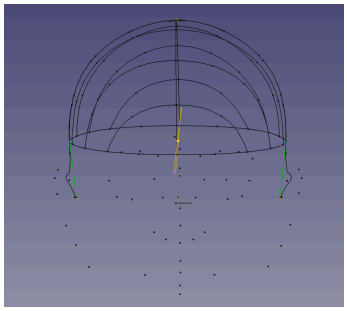

BeamF3 method

The HC, Ns-In and LPA-RPA (cm) are introduced in the BeamF3 web, and the distances X and Y are obtained. The Left Hemisphere wire is converted to a PathArray of 1000 points. By using the rule of three, is determined how many points are needed to advance along the HC line proportionate to the centimeters obtained with the X measurement. Then a plane by the X point, the Cz and the HPCz point is created. A section is created, the sketch is cut and converted to a wire, finally to b-spline and to a path array of 10.000 points. Then, using the Y distance and proportionally to the 10.000 points, the F3 points using the Beam method is located.

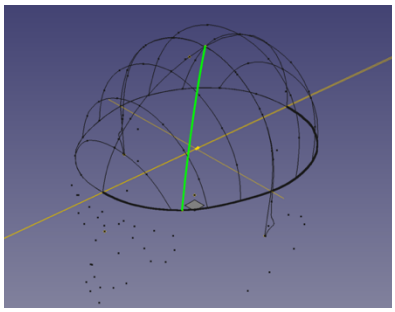

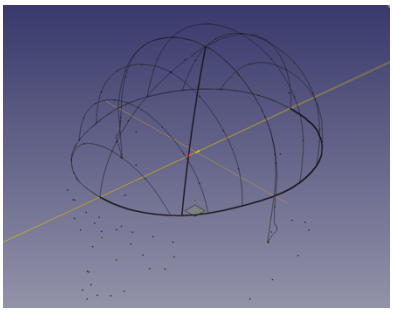

Updated scalp heuristic to locate DLPFC

First, the measures HC, Ns-In and LPA-RPA (cm) are introduced in their equations to obtain the distances X and Y for the 4 different locations (LA, RA, LP and RP). Then, the same procedure as for the BeamF3 method is done (the Path Arrays with 10.000 points and the proportional measures). This is repeated for the 4 points to locate.

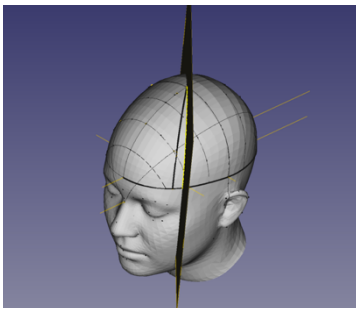

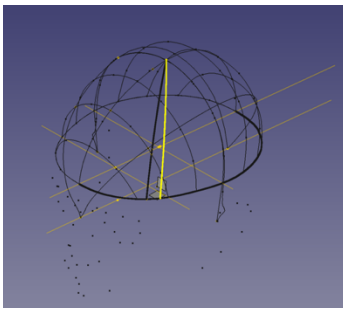

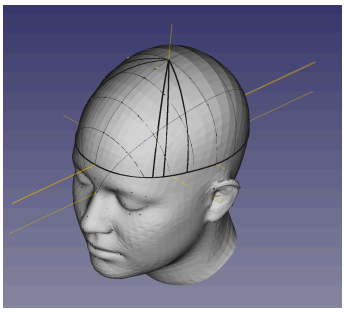

CP3 and CP4 method 5 -7 cm

A cut from Cz to In is created, then a Path Array of 10000 points is generated. By using the rule of three, is determined how many points are needed to advance 5 cm along the line. The point Post 5 cm from Cz is founded.

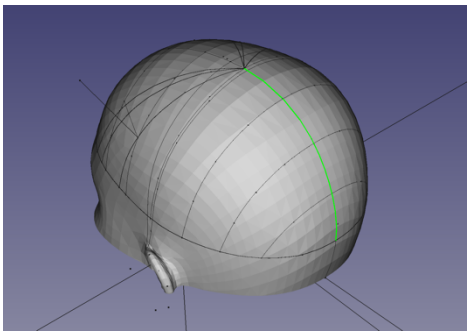
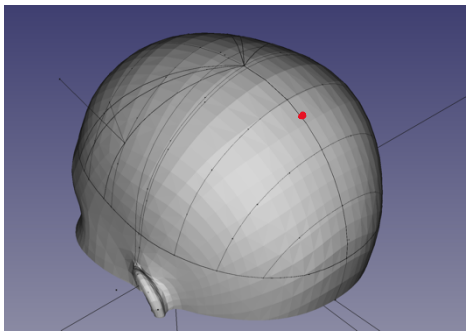

Then a plane with this point, the origin and the Tragus is created. Then is meshed with the head, and a sketch generated. Then two Path Arrays of 10000 points is created (one for each hemisphere) from the Post 5 point to the Tragus. By using the rule of three, is determined how many points are needed to advance 7 cm along the line.

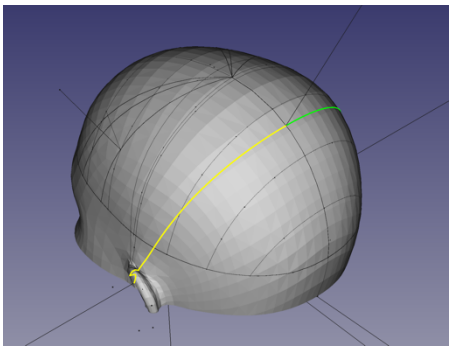
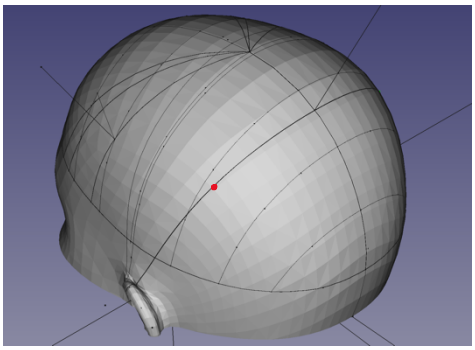

Kocher Point

Five different Kocher Points are created, each of them in the two hemispheres (10 total).

Kocher 1 L/R: 11 cm post Nasion and 3 cm lateral.

A line from Ns to FCz is created, then a Path Array of 10000 points and by the rule of three the relation of how many points are needed to advance 11 cm is calculated. Then this point is marked. Two extra points with the coordinate X of the Post 11 point are created. A plane and an intersection line are generated. Then a Path Array of 10000 points for each lateral, and 3 cm are advanced. Then the K1 Left and Right are founded.

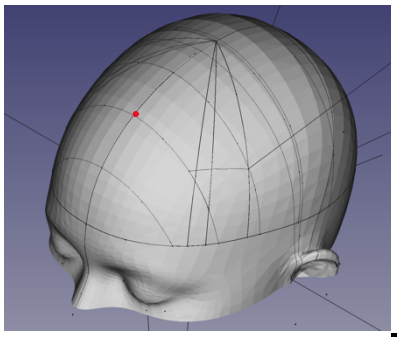
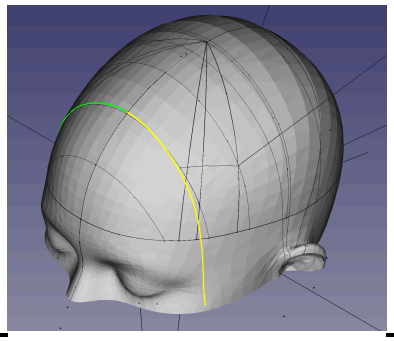
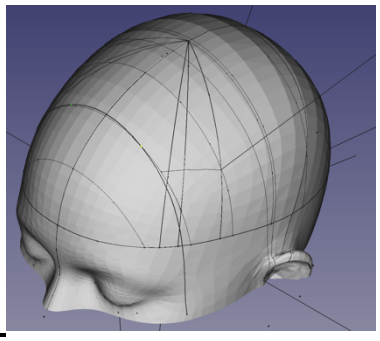

Kocher 2 L/R: 11 cm post Nasion and intersection with Mid Pupillary Line
The Mid Pupillary line is created with the landmark Eye Center Infraorbital left and right, and two other points created with the coordinate Y of this point. Using the post 11 cm point and the lateral Path Array, the intersection of the mid pupillary line and the lateral path array is where the Kocher 2 is located.

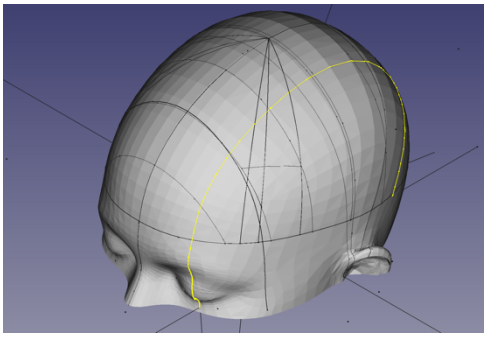
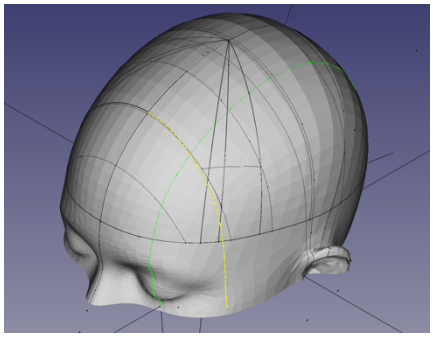

Kocher 3 L/R: FFC3h and FFC4h of the International 10/5 system.
A Path Array of 3 points is created between Fz and FCz. Two other path arrays of 3 points are created between F7 and FT7, and between F8 and FT8. The middle points of each path array are used to create a plane, then is meshed, a sketch is created, and wires at each hemisphere are created. Path arrays of 9 points are created in each hemisphere and the point number 4 is the FFC3h in the left and the FFC4h in the right.

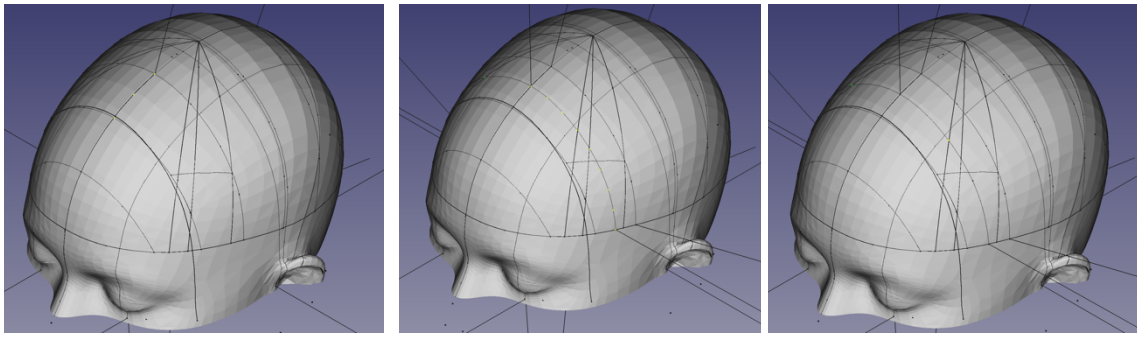

Kocher 4 L/R: Half point between F1 and F3 (L) and between F2 and F4 (R).
A wire from F1 to F3, and a wire from F2 and F4 are created. Then a Path array of 3 points from this wire is generated. The points number 2 of each path array are the Kocher 4 left and right.

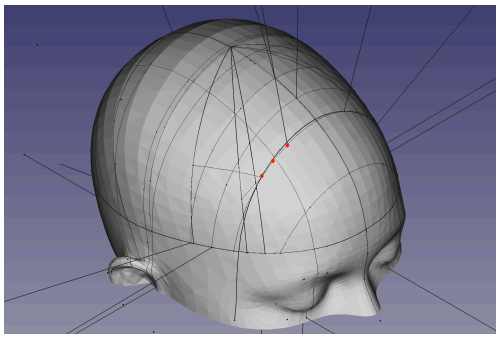
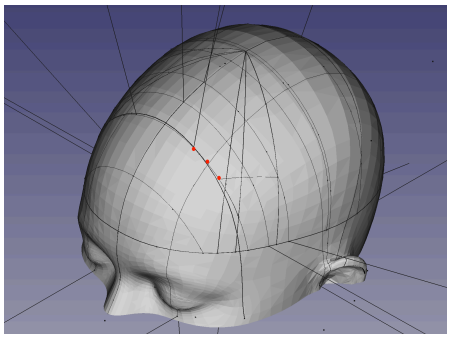

Kocher 5 L/R: 2 cm anterior to coronal suture and intersection with Mid Pupillary line.
A path array of 10000 from the head top symmetric point (in the YZ plane) to Fz is created. Then the relation of 2 cm is calculated, and the 2 cm anterior point is located. Two extra points with the coordinate X of the Anterior 2 point are created. A plane and an intersection line are generated. Then this lateral line is intersected with the Mid Pupillary line, locating the Kocher point 5 left and right.

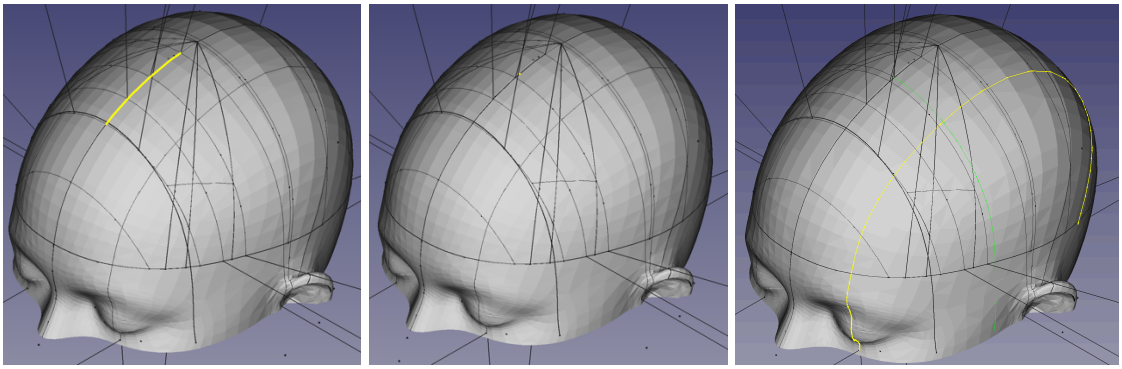

EPlacement measures and relations needed

The data in this section has been removed to maintain confidentiality.

Annex 2 – EPlacement Results

The data in this section has been removed to maintain confidentiality.